JCB Journal of Cell Biology

ARTICLE

Aurora B kinase is recruited to multiple discrete kinetochore and centromere regions in human cells

Amanda J. Broad, Keith F. DeLuca, and Jennifer G. DeLuca

Aurora B kinase has a critical role in regulating attachments between kinetochores and spindle microtubules during mitosis. Early in mitosis, kinase activity at kinetochores is high to promote attachment turnover, and in later mitosis, activity decreases to ensure attachment stabilization. Aurora B localizes prominently to inner centromeres, and a population of the kinase is also detected at kinetochores. How Aurora B is recruited to and evicted from these regions to regulate kinetochore-microtubule attachments remains unclear. Here, we identified and investigated discrete populations of Aurora B at the centromere/kinetochore region. An inner centromere pool is recruited by Haspin phosphorylation of histone H3, and a kinetochore-proximal outer centromere pool is recruited by Bub1 phosphorylation of histone H2A. Finally, a third pool resides ~20 nm outside of the inner kinetochore protein CENP-C in early mitosis and does not require either the Bub1/pH2A/Sgo1 or Haspin/pH3 pathway for localization or activity. Our results suggest that distinct molecular pathways are responsible for Aurora B recruitment to centromeres and kinetochores.

Introduction

During mitotic cell division, chromosomes must equally segregate into two daughter cells so that each new cell has an exact copy of the original genetic material. For this to occur, chromosomes connect to microtubules of the mitotic spindle at structures called kinetochores. In addition to forming kinetochore-microtubule attachments, successful chromosome segregation requires that cells precisely regulate the stability of these attachments (Musacchio and Desai, 2017). In early mitosis, kinetochore-microtubule attachments are short-lived, and microtubule plus ends undergo repeated cycles of attachment and detachment (Cimini et al., 2006; Bakhoum et al., 2009). By maintaining a high level of microtubule turnover in early mitosis, kinetochores ensure that incorrect attachments do not accumulate (Salmon et al., 2005; Godek et al., 2015). As mitosis progresses and chromosomes make their way to the spindle equator, attachments become long-lived, microtubules accumulate at kinetochores, and formation of these stable attachments leads to changes in kinetochore architecture that promote silencing of the spindle assembly checkpoint and anaphase onset (Zhai et al., 1995; Cimini et al., 2006; DeLuca et al., 2006; Etemad and Kops, 2016; Tauchman et al., 2015; Etemad et al., 2015).

A critical regulator of kinetochore-microtubule attachment stability is Aurora B kinase, the enzymatic component of the chromosomal passenger complex (CPC), also comprised of inner centromere protein (INCENP), Survivin, and Borealin (Biggins et al., 1999; Tanaka et al., 2002; Carmena et al., 2012; van der Horst and Lens, 2014; Krenn and Musacchio, 2015). In early mitosis, high Aurora B kinase activity toward kinetochore substrates inhibits the formation of stable microtubule attachments, whereas in late mitosis, low activity promotes stabilization of attachments (Welburn et al., 2010; DeLuca et al., 2011; Zaytsev et al., 2014). A key substrate of Aurora B is Hec1/Ndc80, a member of the four-subunit NDC80 complex and core component of the kinetochore-microtubule attachment interface (Cheeseman et al., 2006; DeLuca et al., 2006). A gradual decrease in phosphorylation of the N-terminal Hec1 unstructured tail domain from early to late mitosis has been implicated in the cumulative stabilization of kinetochore-microtubule attachments (Zaytsev et al., 2014; Zaytsev and Grishchuk, 2015; Yoo et al., 2018).

Aurora B kinase activity toward Hec1 is regulated to ensure that phosphorylation is high on unattached kinetochores and low on those kinetochores that have generated stable attachments to microtubules (DeLuca et al., 2011). A prevailing model to explain this regulation posits that Aurora B is recruited to the inner centromere in early mitosis, and this population of the kinase is responsible for phosphorylating Hec1 and additional outer kinetochore substrates (Liu et al., 2009; Lampson and Cheeseman, 2011). Upon stable attachment to microtubules, as the outer kinetochore is pulled away from the centromere

Department of Biochemistry and Molecular Biology, Colorado State University, Fort Collins, CO.

Correspondence to Jennifer G. DeLuca: jennifer.deluca@colostate.edu.

region by forces generated from microtubule plus end dynamics, the model proposes that Aurora B kinase molecules concentrated at the inner centromere can no longer "reach" outer kinetochore substrates, resulting in their decreased phosphorylation. However, in addition to accumulating at the inner centromere, Aurora B kinase has also been observed at the kinetochore region of mitotic chromosomes, coincident with its kinetochore substrates (Posch et al., 2010; DeLuca et al., 2011). Thus, it is possible that Aurora B is responsible for phosphorylating kinetochore substrates independently of its accumulation at inner centromeres and its distance from this region (Yue et al., 2008; Caldas et al., 2013; Campbell and Desai 2013; Hengeveld et al., 2017; Yoo et al., 2018; Fischböck-Halwachs et al., 2019; García-Rodríguez et al., 2019).

Recruitment of Aurora B and the CPC to the centromere is proposed to depend on two recruitment pathways initiated with distinct histone phosphorylation events. In the first, Haspin kinase phosphorylates histone H3 at Thr3 (T3), which creates a binding site for the CPC component Survivin (Kelly et al., 2010; Wang et al., 2010, 2012; Yamagishi et al., 2010). In the second, Bub1 kinase phosphorylates histone H2A at Thr120 (T120) to recruit the mitotic protein Shugoshin1 (Sgo1), which in turn recruits the CPC, possibly through a linkage to Borealin in human cells (Kawashima et al., 2010; Tsukahara et al., 2010; Yamagishi et al., 2010; Liu et al., 2015). Inhibition of either Haspin or Bub1 and consequent loss of phosphorylated histone H3-T3 (pH3-T3) or phosphorylated H2A-T120 (pH2A-T120), respectively, reduces centromeric accumulation of Aurora B and its CPC partners (Kelly et al., 2010; Wang et al., 2010, 2012; Yamagishi et al., 2010; De Antoni et al., 2012; Bekier et al., 2015; Baron et al., 2016). However, it is not clear how each of these histone marks impact the specific localization patterns and activity of different subpopulations of Aurora B kinase. Therefore in this study, we set out to investigate the role of the Haspin/pH3 and Bub1/pH2A recruitment pathways in Aurora B kinase localization and activity at centromeres and kinetochores of mitotic chromosomes.

Results

pH2A-T120 and pH3-T3 localize to distinct regions within mitotic centromeres

Previous studies have suggested that pH3-T3 and pH2A-T120 exhibit spatial overlap within the centromere of mitotic chromosomes, and this region of overlap is proposed to recruit Aurora B kinase and the rest of the CPC (Yamagishi et al., 2010). However, antibodies to pH3-T3 appear to recognize inner centromeres as a single focus, while antibodies to pH2A-T120 recognize two foci that flank the inner centromere region (Wang et al., 2010; Yamagishi et al., 2010; Kawashima et al., 2010). To further clarify this issue, we tested for colocalization of pH2A-T120 and pH3-T3 in HeLa and U2OS cells in early and late mitosis. We found under all conditions each mark localizes to a discrete region within mitotic chromosomes. pH3-T3 distinctly localizes to the inner centromere as a single focus, whereas pH2A-T120 localizes in a "paired dot" pattern (Fig. 1, A and B). Since this paired dot pattern suggested that phosphorylated histone H2A may localize to kinetochores, we wanted to more precisely determine where within the centromere or kinetochore region H2A is modified. For this we turned to two-color fluorescence localization microscopy (Wan et al., 2009) to map the position of pH2A-T120. We stained cells with antibodies to pH2A-T120, centromere protein C (CENP-C, an inner kinetochore protein), and the N terminus of Hec1 (located in the outer kinetochore; Fig. 1 C). In metaphase cells, our measurements indicate that CENP-C is located 76 ± 10 nm inside of the N terminus of Hec1 (Fig. 1, D and E; Table 1), consistent with previously published work (Wan et al., 2009; Suzuki et al., 2018). Our measurements further revealed that the pH2A-T120 signal is 170 ± 32 nm inside of the N terminus of Hec1 and 95 ± 24 nm inside of CENP-C (Fig. 1, D and E; Table 1). We also analyzed cells in late prophase/early prometaphase (before formation of kinetochore-microtubule attachments) and found that the N terminus of Hec1 was closer to CENP-C in this population of cells (30 ± 9 nm) than in metaphase cells (Fig. 1, D and E; Table 1), which is consistent with previous findings demonstrating that chromosome bi-orientation results in an increase in the inner-to-outer kinetochore distance (Maresca and Salmon, 2009; Uchida et al., 2009). However, we noted that pH2A-T120 remained ~94 nm on the inside of CENP-C in prometaphase cells, similar to its metaphase position (Fig. 1, D and E; Table 1). Together, these results suggest that the centromeric chromatin modified by Bub1 kinase resides significantly inside of the inner kinetochore, but spatially distinct from the inner centromere. Based on these results, we agree that this chromosome region should be referred to as the "kinetochore-proximal outer centromere," as suggested by Hindriksen et al. (2017).

Phosphorylated H3-T3 and H2A-T120 are each capable of recruiting Aurora B kinase and the CPC

Based on the distinct localization patterns of pH3-T3 and pH2A-T120, we tested if each phospho-histone mark was, on its own, sufficient to recruit the CPC. For these experiments, we expressed blue fluorescent protein (BFP)-tagged Haspin kinase or GFP-tagged Bub1 kinase fused to the Lac repressor (LacI) in U2OS cells containing an ectopic Lac operator (LacO) array stably integrated in the short arm of chromosome 1, distant from the centromere (Janicki et al., 2004). As expected, in cells expressing LacI-GFP-Bub1, the chromatin surrounding the LacO array was positive for pH2A-T120 and negative for pH3-T3 (Fig. 2, A and C). In addition, binding of LacI-GFP-Bub1 to the LacO array promoted robust recruitment of Sgo1 (Fig. 2, A and C), consistent with reports demonstrating a pH2A-Sgo1 interaction (Kawashima et al., 2010; Liu et al., 2013, 2015). Also in line with expectations, the chromatin surrounding the LacO array in cells expressing LacI-BFP-Haspin was positive for pH3-T3 and negative for pH2A-T120 (Fig. 2, B and D). Targeting either kinase to the LacO array resulted in robust recruitment of Aurora B kinase and Survivin, indicating that each histone phospho-mark individually is capable of recruiting Aurora B kinase and the CPC in the absence of the other histone modification (Fig. 2). In the case of the Bub1/pH2A pathway, we found that targeting LacI-GFP-Sgo1 to the LacO array was sufficient to supersede the requirement for Bub1 and phosphorylation of H2A in CPC

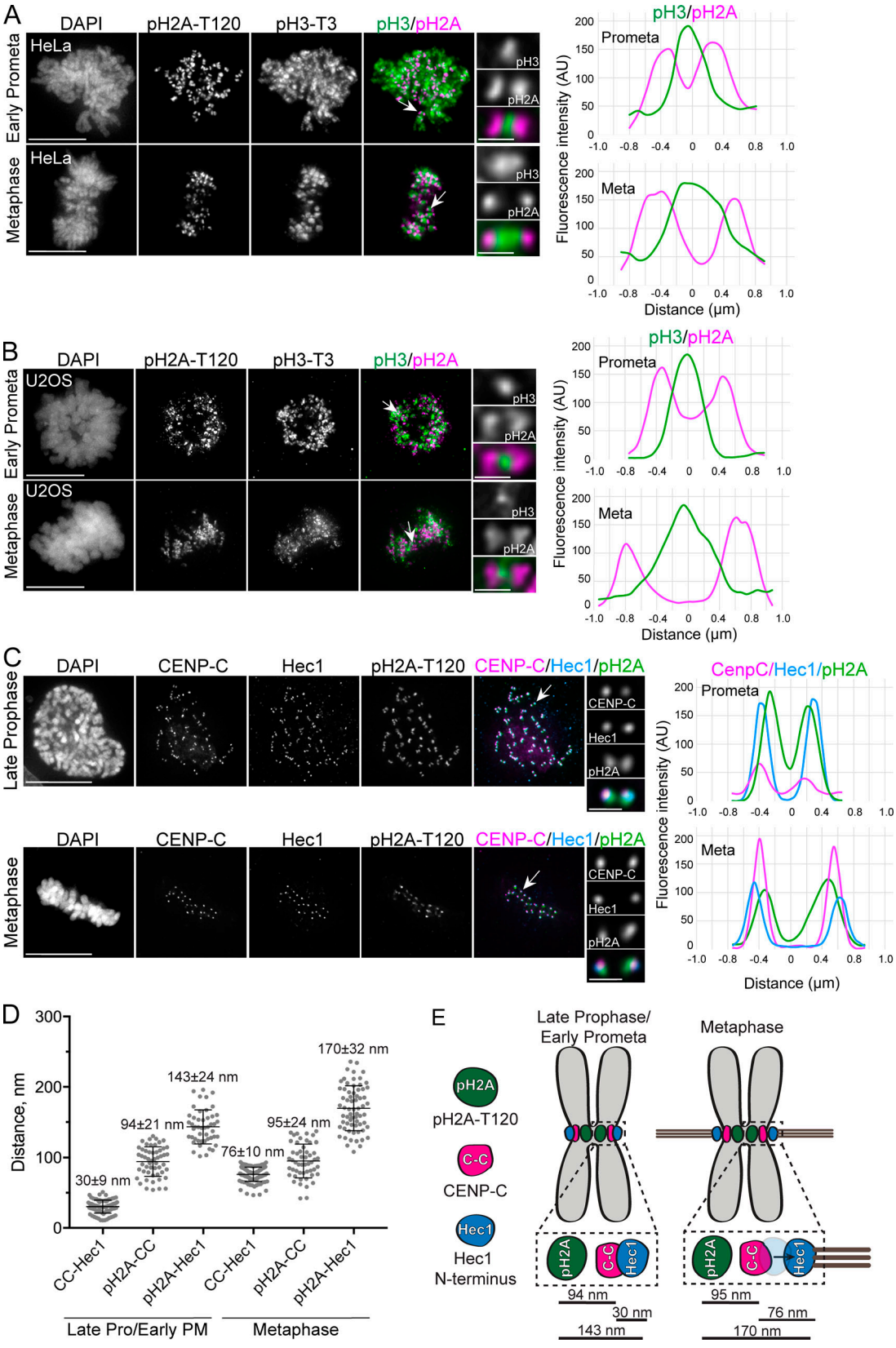

Figure 1. **pH3-T3 and pH2A-T120 occupy discrete locations within the centromere region in mitosis. (A and B)** Immunofluorescence images of early prometaphase and metaphase HeLa (A) and U2OS (B) cells stained with antibodies to phosphorylated histone H3-T3 (pH3) and phosphorylated histone H2A-T120 (pH2A). Arrows point to the kinetochore pairs shown in the insets. Linescans through the centromere/kinetochore region are shown to the right of each panel. **(C)** Immunofluorescence images of late prophase and metaphase HeLa cells stained with antibodies to CENP-C, the N terminus of Hec1 (antibody 9G3), and pH2A-T120. Arrows point to the kinetochore pairs shown in the insets. Linescans through the centromere/kinetochore region are shown to the right of

each panel. **(D)** Plots of the mean distance between the indicated centromere or kinetochore proteins. Each point on the graph represents a distance measurement from a pair of sister chromatids. *n* values are listed in Table 1. Measurements on the left were obtained from late prophase or early prometaphase (PM) HeLa cells; measurements on the right were obtained from metaphase cells. Distance is in nanometers. Error bars represent SD. **(E)** Summary of distance measurements from experiments in C and D. Scale bars, 10 µm (whole cells) and 1 µm (insets). Whole cell images shown are maximum intensity projections of z-stacks containing 64 planes, and inset images shown are projections from 2 to 4 planes. AU, arbitrary units.

recruitment (Fig. S1), in line with previous reports that Sgo1 serves as a bridging factor between pH2A-T120 and the CPC (Kawashima et al., 2010; Liu et al., 2013, 2015). We also found that targeting LacI-GFP-Bub1 to the LacO array failed to promote robust recruitment of Aurora B kinase in cells depleted of Sgo1 (Fig. S1), further supporting the idea that Sgo1 is important for Bub1/pH2A-T120–mediated recruitment of the CPC. Together, our results indicate that each histone phospho-modification is able to recruit the CPC, and raise the possibility that each mark has a unique function in localizing Aurora B kinase to a particular region of the centromere or kinetochore to carry out its roles in regulating mitotic processes.

The Bub1/pH2A-T120/Sgo1 pathway contributes to centromere accumulation of Aurora B but does not contribute to Aurora B kinase activity at the outer kinetochore

Previous studies have demonstrated that depletion of Haspin or Bub1, or inhibition of their respective kinase activities, results in delocalization of Aurora B kinase from the centromere region (Yamagishi et al., 2010; Wang et al., 2012; De Antoni et al., 2012; Baron et al., 2016; Ricke et al., 2011, 2012). Considering that pH2A is proximal to the kinetochore and the Bub1/pH2A-T120/Sgo1 module is capable of recruiting Aurora B kinase independently of Haspin and pH3-T3, we hypothesized that the Bub1/pH2A/Sgo1 pathway may be responsible for recruitment of Aurora B specifically to kinetochores to phosphorylate kinetochore substrates. To test this, we depleted Sgo1 from cells and determined the levels of Aurora B at kinetochores using an antibody to active, phosphorylated Aurora B (pABK-T232) that prominently localizes to outer kinetochores in early mitosis. We found that while centromeric Aurora B levels decreased by ~30% upon Sgo1 depletion (Fig. 3, A and B), which is consistent with previous reports (Kawashima et al., 2007; Meppelink et al., 2015), pABK-T232 levels were unchanged after Sgo1 depletion (Fig. 3, C and D). Furthermore, depletion of Sgo1 did not reduce phosphorylation of Hec1-S44, a known Aurora B kinase kinetochore substrate (DeLuca et al., 2011; Fig. 3, E and F), indicating that the activity of Aurora B at kinetochores remains high in spite of perturbation of the Bub1/pH2A/Sgo1 recruitment pathway. Consistent with these results, overexpression of wild-type (WT) Sgo1, or mutant versions of Sgo1 that either cannot bind cohesin and localize primarily to kinetochores (Sgo1-T346A), or cannot bind pH2A-T120 and localize primarily to chromosome arms (Sgo1-K492A; Liu et al., 2013), did not drive accumulation of kinetochore-associated pABK-T232 or lead to an increase in phosphorylation of Hec1-S44 (Fig. 3, I–N). These results suggest, contrary to our hypothesis, that while the Bub1/pH2A/Sgo1 pathway contributes to the localization of Aurora B kinase at the centromere, it does not significantly impact recruitment or activity of kinetochore-associated Aurora B kinase. These results also support the idea that loss of centromere-associated Aurora B does not strictly correlate to a reduction in Aurora B kinase activity at the kinetochore (Yue et al., 2008; Caldas et al., 2013; Campbell and Desai, 2013; Trivedi et al., 2019).

Bub1 depletion partially reduces Aurora B kinase activity at outer kinetochores

It has been previously established that Bub1 kinase is required for efficient accumulation of Aurora B at centromeres through the Bub1/pH2A/Sgo1 recruitment pathway (Kelly et al., 2010;

Table 1. **Mean distance measurements for kinetochore and centromere components described in Figs. 1 and 6**

	Distance, nm	SD	# Kinetochores	# Cells
Metaphase				
CENP-C to Hec1 N-term	76.2	10.2	113	19
pH2A to CENP-C	95.1	24.1	52	10
pH2A to Hec1 N-term	170.0	31.8	67	10
Late prophase/early prometaphase				
CENP-C to Hec1 N-term	30.4	9.3	86	18
pH2A to CENP-C	94.4	20.9	51	10
pH2A to Hec1 N-term	143.4	24.0	67	10
CENP-C to pABK	21.8	11.8	51	15
ABKGFP to CENP-C	64.7	39.4	96	27
ABKGFP to Hec1 N-term	107.4	48	81	22

Shown for each are the average distances, SDs, and number of kinetochores/centromeres and cells measured for each condition.

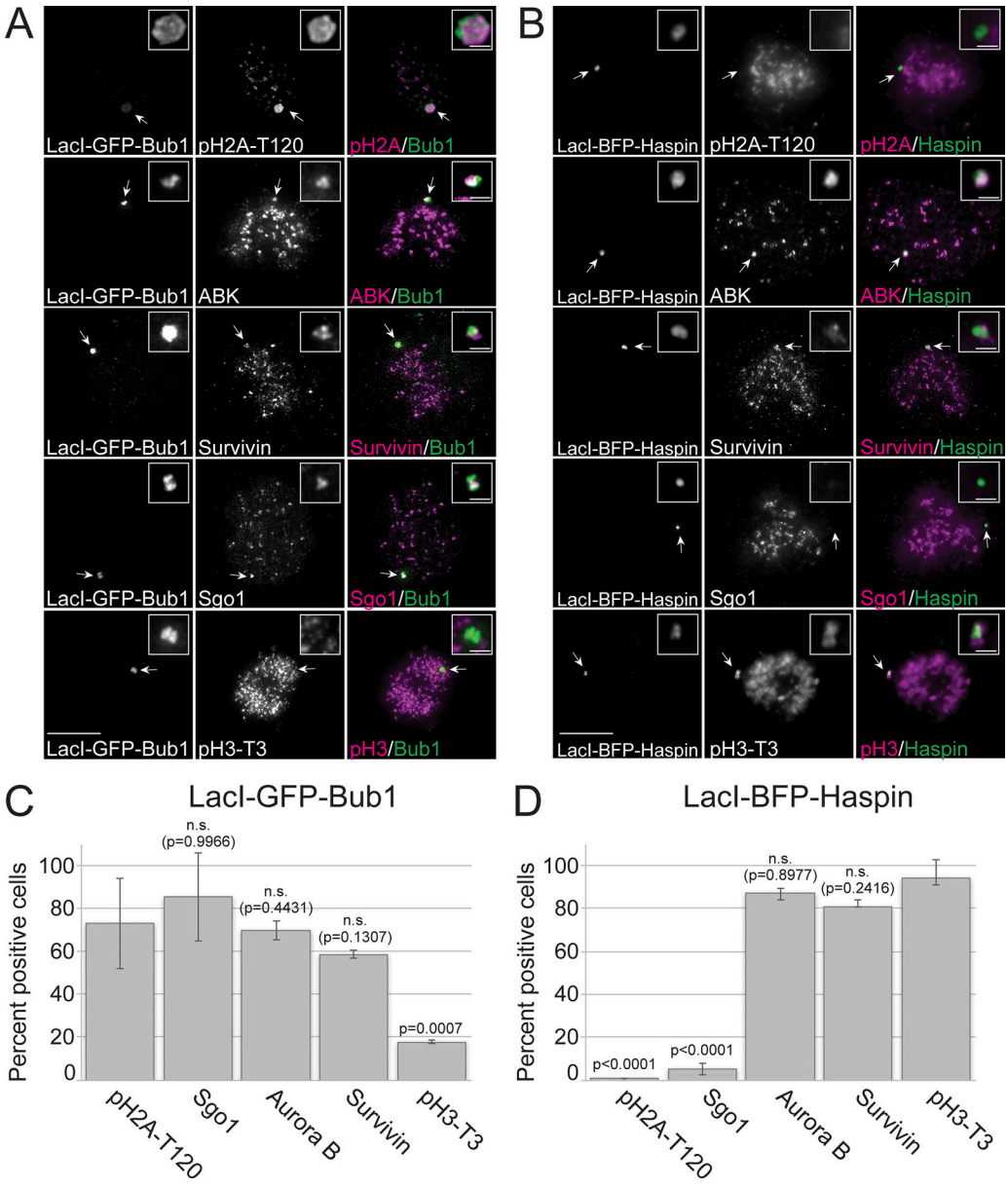

Figure 2. **pH3-T3 and pH2A-T120 are each capable of recruiting Aurora B kinase and the CPC. (A and B)** Immunofluorescence images of U2OS cells expressing LacI-GFP-Bub1 (A) or LacI-BFP-Haspin (B). Cells were immunostained for the indicated centromere/kinetochore proteins or phospho-specific epitopes. Arrows point to the LacO array with indicated LacI-fused protein shown in the insets. Cells were synchronized in G2 using RO-3306 and washed out of drug 30 min before fixation to enrich for early mitotic cells. **(C and D)** Quantification of experiments in A and B. The average fluorescence intensity of each antibody was measured at the LacO array in cells expressing either LacI-BFP or LacI-GFP (not fused to a test protein), and average values were measured and used to calculate thresholds. Fluorescence intensities of each antibody were then measured in cells expressing LacI-BFP-Haspin or LacI-GFP-Bub1, and cells were scored as positive if intensity values were higher than the calculated thresholds. For each experiment, ≥20 cells were quantified from $n \geq 3$ experiments. Error bars represent SD. Significance values were calculated from a one-way ordinary ANOVA test. Shown are significance values between experiments for each test antibody and either pH2A-T120 (C) or pH3-T3 (D). Scale bars, 10 µm (whole cells) and 1 µm (insets). n.s., not significant.

Wang et al., 2010, 2012; Yamagishi et al., 2010; De Antoni et al., 2012; Baron et al., 2016; Ricke et al., 2012). Consistent with these studies, we find that Bub1 depletion results in a decrease in centromere-associated Aurora B kinase by ~55% compared with levels measured in control cells (Fig. S2). The remaining 45% of centromere Aurora B is presumably recruited through the Haspin/pH3-T3 pathway (see below and Fig. S5). We also tested if depletion of Bub1 affected kinetochore-associated Aurora B kinase and found that in cells treated with Bub1 siRNA, levels of pABK-T232 and pHec1-S44 at kinetochores were reduced to ~30% of levels measured in control cells (Fig. S2; Caldas et al., 2013). Since depletion of Bub1 reduced the level of Aurora B kinase activity at kinetochores, we asked if this reduction was specifically due to loss of Bub1's kinase activity. To this end, we treated cells with a Bub1 inhibitor, BAY320, at 10 µM, which was sufficient to inhibit phosphorylation of H2A-T120, but had no effect on phosphorylation of H3-T3 (Fig. S4; Baron et al., 2016). As shown in Fig. 4 A, and consistent with prior results,

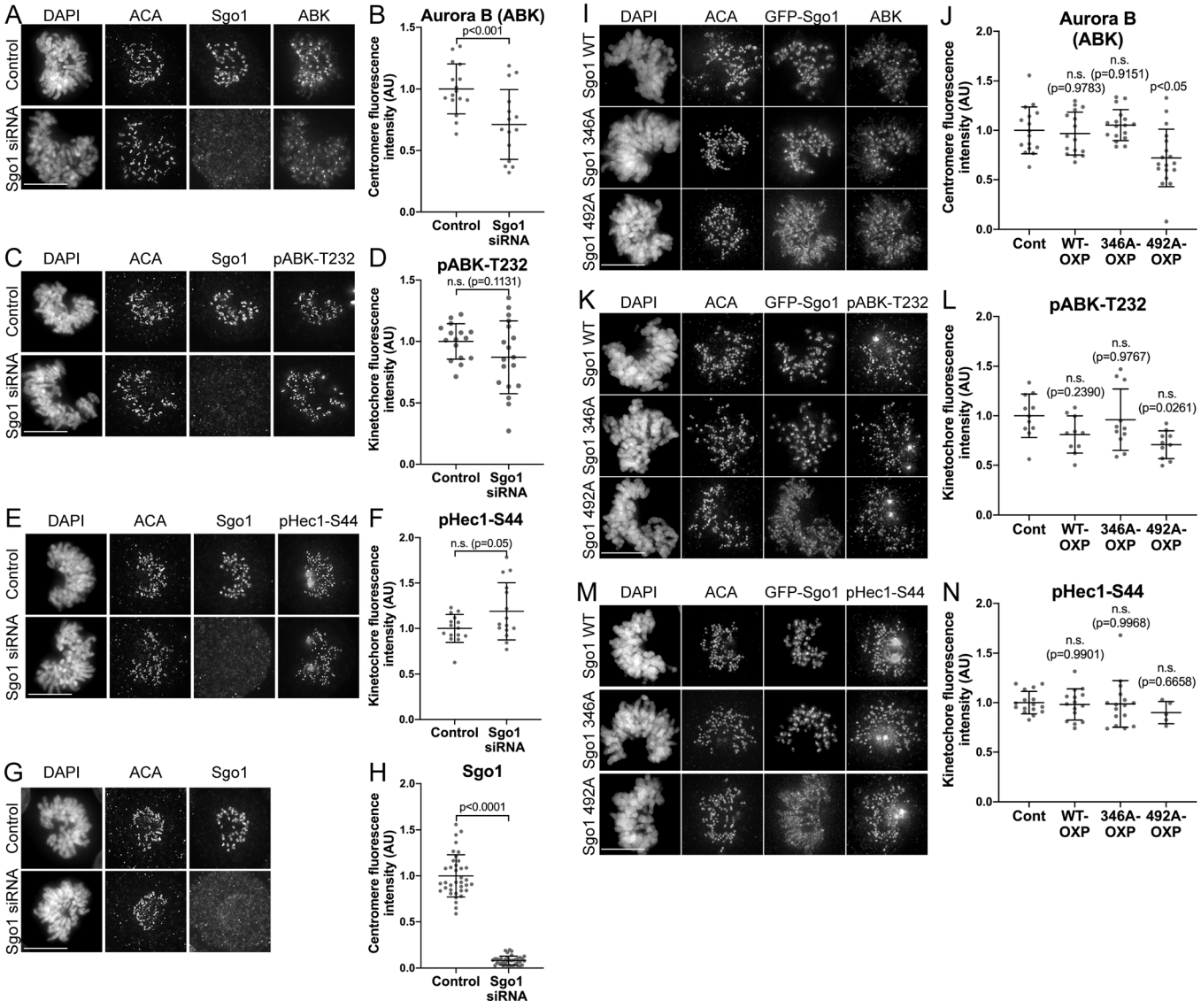

Figure 3. **The Bub1/pH2A-T120/Sgo1 pathway contributes to the accumulation of centromere-associated Aurora B but not localization or activity of kinetochore-associated Aurora B. (A, C, E, and G)** Immunofluorescence images of HeLa cells depleted of Sgo1 and stained for either Aurora B (ABK), active phosphorylated ABK (pABK-T232), phosphorylated Hec1-S44 (pHec1-S44), or Sgo1. **(B, D, F, and H)** Quantification of centromere or kinetochore fluorescence intensities of Aurora B, pABK-T232, pHec1-S44, and Sgo1. For all conditions, at least 120 kinetochores from 10 cells were measured from a total of three independent experiments. Fluorescence intensities for Sgo1 depletion were normalized to those calculated from control cells. **(I, K, and M)** HeLa Flp-In TREx cells were induced to express GFP-Sgo1-WT, GFP-Sgo1-K492A, or GFP-Sgo1-T346A fusion proteins (Liu et al., 2013) and immunostained for ABK, pABK-T232, or pHec1-S44. **(J, L, and N)** Quantification of centromere (ABK) or kinetochore (pABK-T232, pHec1-S44) normalized fluorescence intensities. For ABK quantification, 120 centromeres were measured from 15 cells from three independent experiments. For pABK-T232 and pHec1-S44, at least 200 kinetochores were measured from at least 15 cells from three independent experiments. Fluorescence intensities for test conditions were normalized to those calculated from control cells. Error bars represent SD. For B, D, F, and H, significance values were calculated from unpaired nonparametric Student's *t* tests. For J, L, and N, significance values were calculated from a one-way ordinary ANOVA test, and shown are significance values between experiments using cells overexpressing WT or mutant Sgo1 constructs compared with control, untreated cells. AU, arbitrary units; ACA, anti-centromere antibody. Scale bars, 10 µm.

centromere accumulation of Aurora B was reduced after BAY320 treatment to ~68% of control levels (Baron et al., 2016). To determine if activity of centromeric Aurora B was affected by this loss of accumulation, we generated and stained cells with a phospho-specific antibody to the TSS (Thr892/Ser893/Ser894) motif of human INCENP (Fig. S3), a well-characterized Aurora B substrate (Bishop and Schumacher, 2002; Sessa et al., 2005; Wang et al., 2012). Cells inhibited for Bub1 kinase activity exhibited a modest reduction in pINCENP-S893, S894 levels at centromeres (to ~77% of control levels), suggesting that the Aurora B recruited to centromeres via the Haspin/pH3-pathway retains activity (Fig. 4 B). We then tested if the activity of Aurora B at kinetochores was reduced upon kinase inhibition of Bub1. Kinetochore-associated pABK-T232 levels remained high in cells treated with BAY320 (Fig. 4 C), and consistent with this result, phosphorylation of Aurora B kinetochore substrates pHec1-S44 and pKnl1-S24 were not significantly decreased by treatment with BAY320 (Fig. 4, D and E). We did note a small but

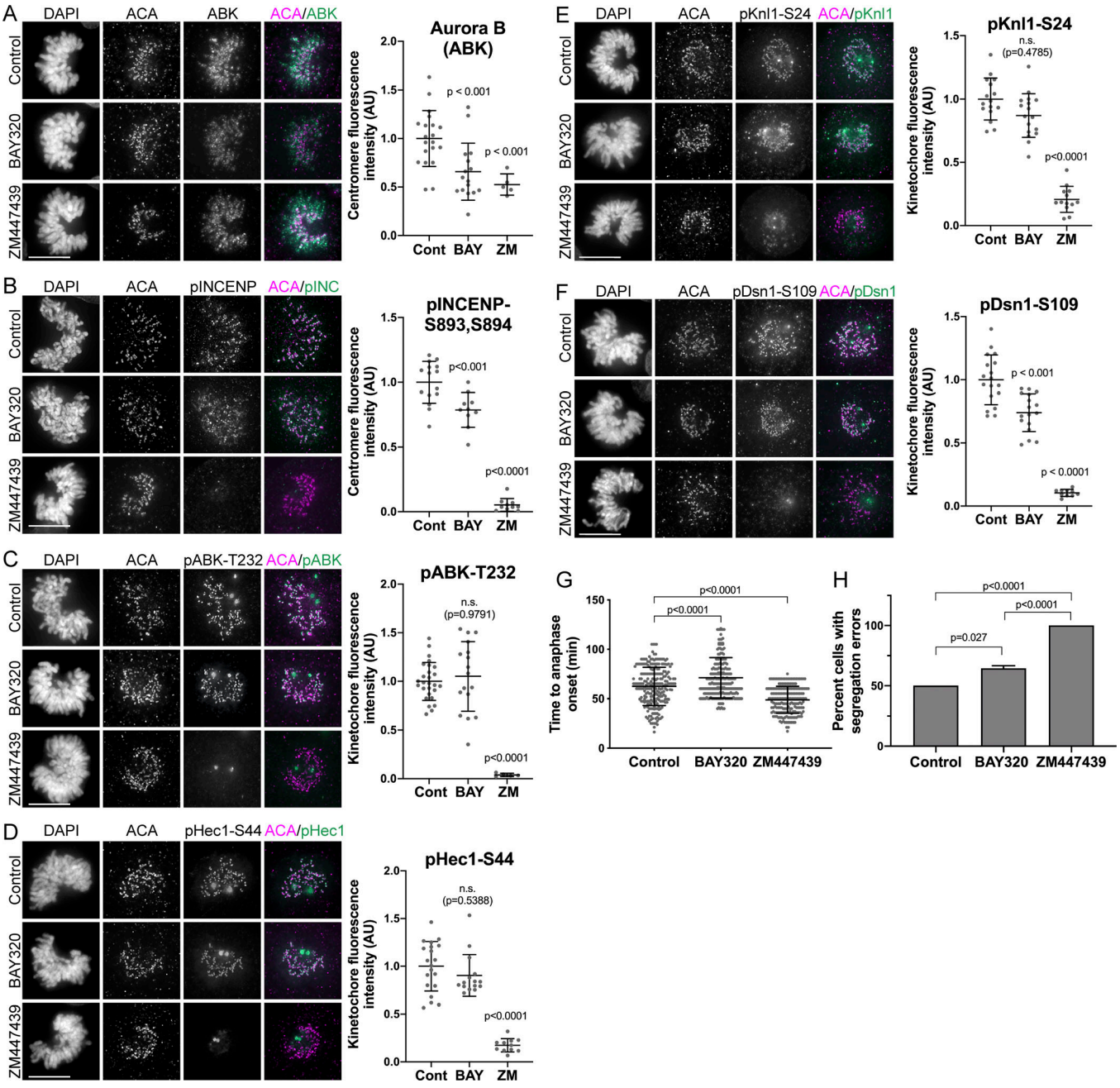

Figure 4. **Bub1 kinase activity is not required for localization or activity of Aurora B at kinetochores. (A–F)** Immunofluorescence images of control HeLa cells or HeLa cells treated with either 10 µM Bub1 kinase inhibitor BAY320 or 20 µM Aurora B kinase inhibitor ZM447439. Cells were fixed and stained with the indicated antibodies. To the right of each immunofluorescence panel is the quantification of centromere or kinetochore fluorescence intensity. Fluorescence intensities for test conditions were normalized to those calculated from control cells. *n* values for each experiment follow. ABK: Control (*n* = 153 centromeres; 15 cells; three experiments); BAY320 (*n* = 226 centromeres; 13 cells; four experiments); ZM447439 (*n* = 222 centromeres; 11 cells; three experiments). pINCENP: Control (*n* = 349 centromeres; 15 cells; three experiments); BAY320 (*n* = 245 centromeres; 10 cells; three experiments); ZM447439 (*n* = 179 centromeres; 10 cells; three experiments). pABK-T232: Control (*n* = 621 kinetochores; 42 cells; four experiments); BAY320 (*n* = 350 kinetochores; 24 cells; four experiments); ZM447439 (*n* = 219 kinetochores; 6 cells; three experiments). pHec1-S44: Control (*n* = 384 kinetochores; 16 cells; three experiments); BAY320 (*n* = 272 kinetochores; 15 cells; three experiments); ZM447439 (*n* = 224 kinetochores; 11 cells; three experiments). pKnl1-S24: Control (*n* = 363 kinetochores; 16 cells; three experiments); BAY320 (*n* = 348 kinetochores; 17 cells; three experiments); ZM447439 (*n* = 281 kinetochores; 14 cells; three experiments). pDsn1-S109: Control (*n* = 400 kinetochores; 18 cells; three experiments); BAY320 (*n* = 368 kinetochores; 17 cells; three experiments); ZM447439 (*n* = 209 kinetochores; 10 cells; two experiments). **(G)** Quantification of time (in min) to anaphase onset after washout of monastrol. HeLa cells were treated with 150 µM monastrol for 2 h. Cells were washed out into control media, or media containing either 10 µM BAY320 or 20 µM ZM447439. The time from initiation of washout to anaphase onset was scored. For each condition, at least 200 cells were quantified from three experiments. **(H)** Quantification of chromosome segregation errors in cells treated with 150 µM monastrol for 2 h, and washed out into control media, or media containing either 10 µM BAY320 or 20 µM ZM447439. Errors in chromosome segregation were quantified from anaphase cells. For A-F, significance values were calculated from unpaired nonparametric Student's *t* tests. For G and H, significance values were calculated from one-way ordinary ANOVA tests. AU, arbitrary units; Cont, control; BAY, BAY320; ZM, ZM447439. Scale bars, 10 µm.

significant decrease in phosphorylation of Dsn1-S109, an Aurora B kinase target site that is implicated in kinetochore assembly rather than error correction (Akiyoshi et al., 2013; Kim and Yu, 2015; Rago et al., 2015; Zhou et al., 2017; Hara et al., 2018), to ~75% of control levels (Fig. 4 F). In contrast, treatment of cells with ZM447439, an Aurora B kinase inhibitor (Ditchfield et al., 2003; Wang et al., 2012), resulted in a near-complete loss of kinetochore-associated pABK-T232, pHec1-S44, pKnl1-S24, pINCENP-S893, S894, and pDsn1-S109 (Fig. 4, D–F). Finally, we tested the efficiency of error correction in the presence of BAY320 using a monastrol washout assay. In this assay, cells are arrested in monastrol, which results in the formation of monopolar spindles containing a large number of attachment errors in which both sister kinetochores are attached to the single spindle pole (Kapoor et al., 2000). Upon washout of monastrol, bipolar spindles form, attachment errors are corrected in an Aurora B kinase-dependent manner, and chromosomes eventually align to the spindle equator and separate at anaphase (Lampson and Kapoor, 2005). To determine if loss of Bub1 kinase activity affects attachment error correction, we measured both the time from monastrol washout to anaphase onset and the percentage of cells exhibiting chromosome segregation errors in cells treated with BAY320. As expected, upon inhibition of Aurora B kinase with the small molecule ZM447439, error correction was severely impaired and cells entered anaphase, on average, 49 min after monastrol washout with a large number of uncorrected, erroneous attachments, resulting in severe chromosome segregation defects (Fig. 4, G and H). Consistent with our finding that phosphorylation of kinetochore-associated Aurora B substrates are unaffected by Bub1 kinase inhibition, we did not observe statistically significant changes in the rate of chromosome segregation errors in the presence of BAY320 after monastrol washout or in the timing of anaphase onset compared with control cells (Fig. 4, G and H), suggesting the presence of an intact error correction system. These results suggest that although Bub1 kinase activity is required for efficient centromere localization of Aurora B, it does not contribute to Aurora B activity at kinetochores. In contrast, depletion of the Bub1 protein from mitotic cells resulted in a decrease in kinetochore-associated Aurora B activity (Fig. S2), which, together with the BAY320 experiments, suggests that Bub1, but not its kinase function, contributes to either the recruitment or activity of Aurora B at the kinetochore.

Inhibition of Haspin kinase relocalizes Aurora B from inner centromeres to kinetochore-proximal outer centromeres

Our results thus far suggest that although the Bub1/pH2A/Sgo1 pathway promotes efficient accumulation of Aurora B at the centromere, it is not required for localization or activity of Aurora B at kinetochores. This led us to ask if the Haspin/pH3 pathway, which is also required for efficient accumulation of Aurora B at the centromere (Kelly et al., 2010; Wang et al., 2010, 2012; Yamagishi et al., 2010), is important for localization or activity of Aurora B at kinetochores. We therefore treated cells with the Haspin inhibitor, 5-iodotubercidin (5-ITu), and assessed recruitment of pABK-T232 to kinetochores and phosphorylation of multiple kinetochore Aurora B substrates. Unfortunately, addition of the inhibitor at concentrations that resulted in full inhibition of Haspin kinase activity toward pH3-T3 (1–10 µM; De Antoni et al., 2012; Wang et al., 2012; Bekier et al., 2015) resulted in decreased activity of Bub1 kinase, suggesting that the inhibitor exhibits some degree of non-specificity at the concentrations used (Fig. S4; De Antoni et al., 2012; Bekier et al., 2015). Even so, we found that while treatment of cells with both 10 µM BAY320 and 10 µM 5-ITu led to a complete loss of accumulation and activity of Aurora B at the centromere (Fig. S5), levels of kinetochore pABK-T232 were not decreased (Fig. S5). Furthermore, phosphorylation levels of kinetochore-associated Aurora B kinase substrate Knl1-S24 were not significantly reduced, and Hec1-S44 phosphorylation levels were only modestly decreased (Fig. S5). Interestingly, we did measure a decrease in phosphorylation of Dsn1-S109 (an Aurora B kinase substrate implicated in kinetochore assembly) to ~45% of control levels upon treatment of cells with both BAY320 and 5-ITu (Fig. S5). We note that in an accompanying manuscript by Hadders et al. (2020), the authors report that phosphorylation levels of Dsn1-S109 are not reduced in Haspin knock-out cells or in Haspin knock-out cells treated with the Bub1 inhibitor BAY320. These findings suggest, consistent with our earlier results, that 5-ITu may induce off-target effects that differentially affect kinetochore functions at the concentrations required to inhibit Haspin activity in cells.

We noted that after treatment with 5-ITu and loss of centromere-localized Aurora B, a population of Aurora B, detected in cells expressing Aurora B-GFP, relocalized from the inner centromere to a "double dot" pattern, reminiscent of what we observed for pH2A-T120 staining (Fig. 1). Linescans of kinetochore pairs from cells treated with 5-ITu suggest that this population of Aurora B resides inside of both inner and outer kinetochore markers (Fig. 5, A and B). Indeed, we confirmed this by measuring the distances between Aurora B-GFP and both CENP-C and the N terminus of Hec1. After 5-ITu treatment in early mitotic cells, Aurora B–GFP localizes 65 ± 39 nm inside of CENP-C and 107 ± 48 nm inside of the N terminus of Hec1 (Fig. 6, C and D; Table 1). Therefore, after loss of the pH3-T3 binding site in the inner centromere, Aurora B kinase is still recruited to the kinetochore-proximal outer centromere, likely through the Bub1/pH2A/Sgo1 pathway (Fig. S5).

Aurora B kinase and INCENP localize to both centromeres and kinetochores in mitotic cells

Two distinct pathways contribute to accumulation of Aurora B kinase at centromeres; however, neither of these pathways impacts Aurora B localization at kinetochores. These data suggest that the population of Aurora B at the kinetochore may be not only functionally but also spatially distinct from both the inner centromere and kinetochore-proximal outer centromere populations of the kinase. To test this, we mapped the position of what we hypothesized to be "kinetochore-localized" Aurora B. Indeed, our measurements indicate that a population of Aurora B detected by the pABK-T232 antibody resides within the kinetochore proper and is on average ~22 nm outside of CENP-C, and ~8 nm inside of the N terminus of Hec1 in early mitosis (Fig. 6, A, C, and D; Table 1).

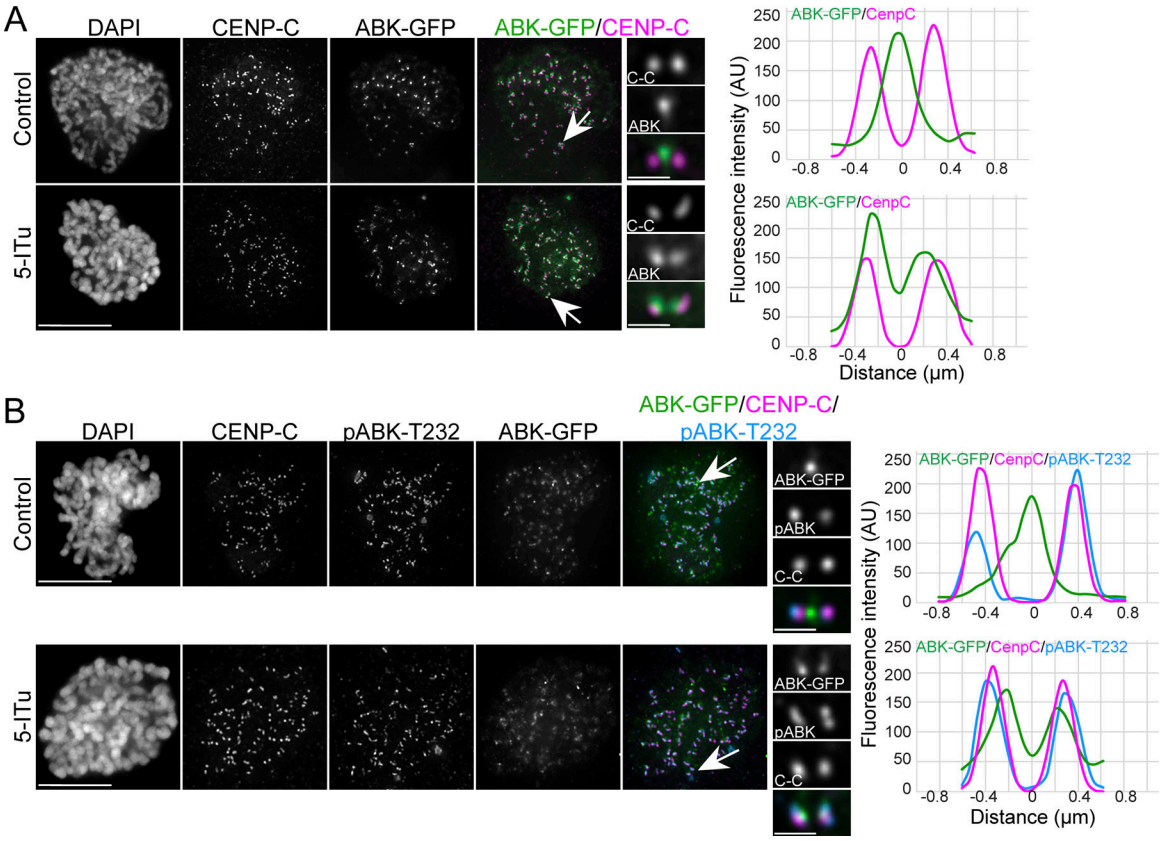

Figure 5. **Inhibition of Haspin kinase results in relocalization of Aurora B from inner centromeres to kinetochore-proximal outer centromeres. (A)** Immunofluorescence images of control and 5 µM 5-ITu-treated early prometaphase HeLa cells expressing Aurora B kinase-GFP (ABK-GFP) and stained with antibodies to CENP-C. Arrows point to the kinetochore pairs shown in the insets. Linescans through the centromere/kinetochore region are shown to the right of each panel. **(B)** Immunofluorescence images of control and 5 µM 5-ITu-treated early prometaphase HeLa cells expressing ABK-GFP and stained with antibodies to pABK-T232. Arrows point to the kinetochore pairs shown in the insets. Linescans through the centromere/kinetochore region are shown to the right of each panel. Scale bars, 10 µm (whole cells) and 1 µm (insets). Whole cell images shown are maximum intensity projections of z-stacks containing 64 planes, and inset images shown are projections from 2 to 4 planes. AU, arbitrary units.

Finally, to confirm that the multiple populations of Aurora B detected at the centromere and kinetochore region are components of active CPC complexes, we stained cells with a phospho-specific antibody to INCENP (pINCENP-S893, S894), whose phosphorylation is required for activation of Aurora B and serves as an indicator of CPC activity (Bishop and Schumacher, 2002; Sessa et al., 2005). In late prometaphase and metaphase, pINCENP-S893, S894 localized prominently to the inner centromere, as previously reported (Salimian et al., 2011; Fig. S3). However, in early mitosis, we observed pINCENP-S893, S894 at multiple locations within the centromere and kinetochore. In the majority of kinetochore pairs, we observed robust localization of pINCENP-S893, S894 at the outer kinetochore (as determined by linescans), confirming that the outer kinetochore-localized Aurora B is indeed active (Fig. 6 B). In addition, although less frequently, we were able to detect populations of pINCENP-S893, S894 at the inner centromere and the kinetochore-proximal outer centromere in early mitotic cells (Fig. 6 B). Since pINCENP-S893, S894 localized to all three localizations, we were unable to accurately map its precise location within the centromere and/or kinetochore using a two-color fluorescence localization approach.

Discussion

Aurora B kinase localizes prominently to the inner centromere during mitosis. Several of its known substrates also localize to this region including its activator, INCENP, and the kinesin-13 microtubule motor protein MCAK, both of which have important roles in mitotic progression (Andrews et al., 2004; Lan et al., 2004; Bishop and Schumacher, 2002; Sessa et al., 2005). Additionally, a population of Aurora B has been detected at the outer kinetochore in early mitosis, where it is proposed to have a role in phosphorylating substrates that regulate kinetochore-microtubule attachment stability (Posch et al., 2010; DeLuca et al., 2011; Yoo et al., 2018). Resolving how Aurora B is recruited to each of these regions is critical to understand how the kinase is regulated temporally during mitosis so that erroneous kinetochore-microtubule attachments are corrected and proper attachments are stabilized. Previous studies have shown that Aurora B and the CPC are recruited to centromeres through two phospho-histone modifications generated by Haspin-mediated phosphorylation of histone H3-T3 and Bub1-mediated phosphorylation of histone H2A-T120 (Kelly et al., 2010; Wang et al., 2010, 2012; Yamagishi et al., 2010; Kawashima et al., 2010; Tsukahara et al., 2010; Liu et al., 2015; Watanabe, 2010). Both

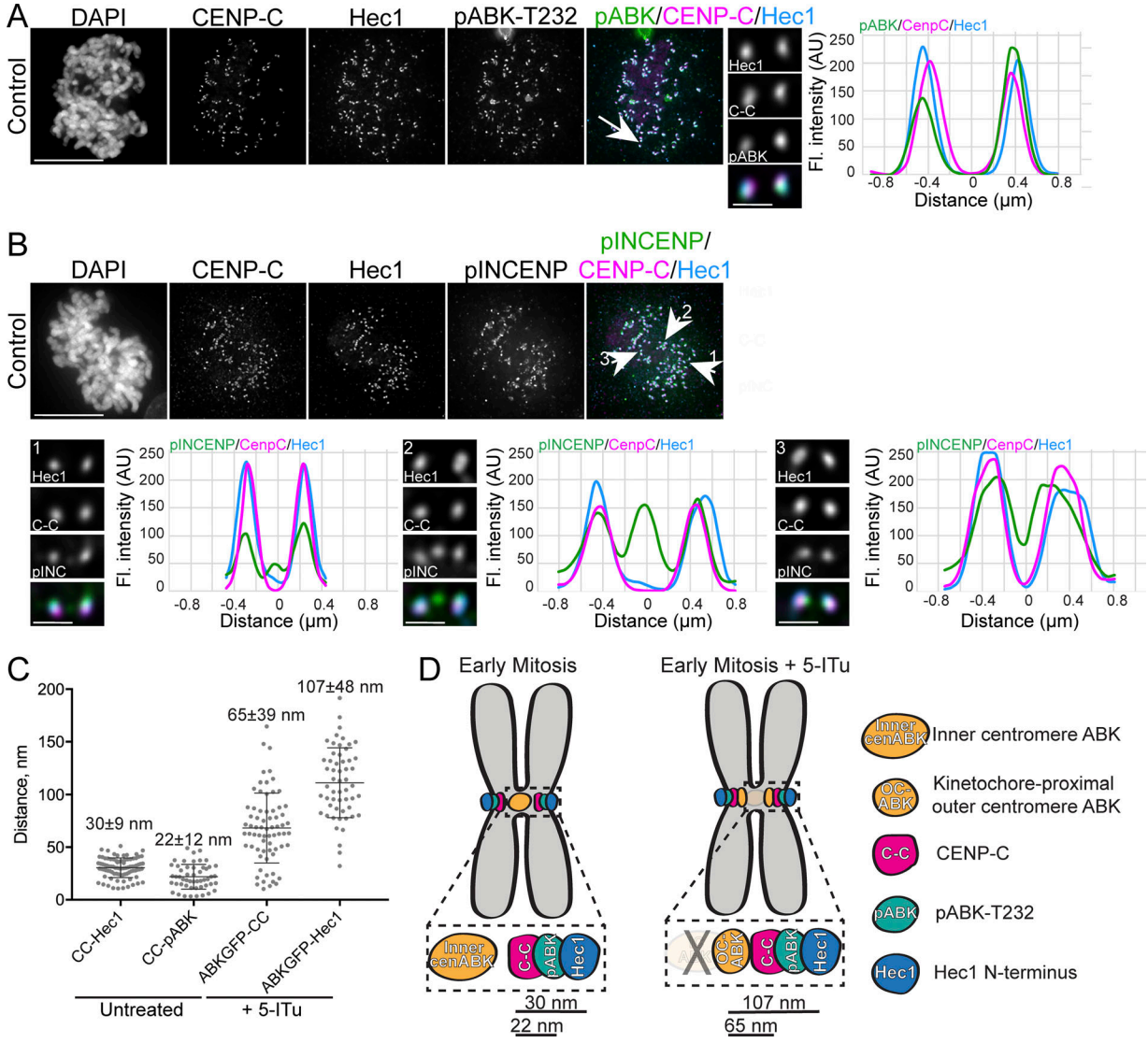

Figure 6. **Aurora B kinase and INCENP localize to both centromeres and kinetochores in mitotic cells. (A)** Immunofluorescence images of an early prometaphase control HeLa cell stained with antibodies to pABK-T232, CENP-C, and the N-terminus of Hec1 (antibody 9G3). Arrows point to the kinetochore pairs shown in the insets. A linescan through the centromere/kinetochore region is shown to the right of the panel. **(B)** Immunofluorescence images of an early prometaphase control HeLa cell stained with antibodies to pINCENP, CENP-C, and the N terminus of Hec1 (antibody 9G3). Numbers indicate kinetochore pairs shown in the insets, and linescans through the centromere/kinetochore region are shown to the right of each panel. pINCENP is localized to the kinetochore (pair 1), the centromere and kinetochore (pair 2), or the kinetochore-proximal outer centromere (pair 3). **(C)** Plots of the mean distance between the indicated proteins. Each point on the graph represents a distance measurement for a pair of sister chromatids, and the mean value is indicated. Error bars indicate SD. *n* values are listed in Table 1. **(D)** Summary of distance measurements from experiments in the study. Scale bars, 10 µm (whole cells) and 1 µm (insets). Whole cell images shown are maximum intensity projections of z-stacks containing 64 planes, and inset images shown are projections from 2 to 4 planes. Fl. intensity is fluorescence intensity; AU, arbitrary units.

modifications are required for efficient Aurora B accumulation at centromeres, and it has been suggested that the region within the centromere where both phospho-marks overlap serves as the recruitment site for the CPC (Yamagishi et al., 2010; Watanabe, 2010). However, we found that in both HeLa and U2OS cells in early and late mitosis, these two phosphohistone modifications are spatially distinct, with pH3-T3 localized to the inner centromere and pH2A-T120 localized to the kinetochore-proximal outer centromere. Additionally, both modifications are individually capable of recruiting Aurora B and CPC components, indicating that explicit overlap of the two marks within centromeric chromatin is not required for CPC recruitment. Based on these results, we hypothesized that the kinetochore-proximal outer centromere population of the CPC recruited by phospho-H2A might be responsible for the localization and activity of Aurora B at kinetochores. We discovered, however, that this is not the case and the Bub1/pH2A/Sgo1 pathway is not required for kinetochore localization or activity of Aurora B. Rather, both histone marks, although spatially distinct, contribute to accumulation of Aurora B and the CPC at the centromere (Fig. 5, A and B).

We found that in early mitosis, Aurora B, detected by a pan-Aurora B antibody, localizes predominantly to the inner centromere, and we rarely observed localization at the kinetochore-proximal outer centromere (Fig. 5, A and B). However, upon inhibition of Haspin kinase with 5-ITu (which decreases but does not completely eliminate Bub1 kinase activity), Aurora B localizes prominently to the kinetochore-proximal outer centromere region in early mitotic cells (Fig. 5, A and B). A similar relocalization pattern was observed for the CPC component Borealin in cells treated with 5-ITu (Bekier et al., 2015). Based on these findings, we speculate that Aurora B and the CPC are recruited to the outer centromere region transiently. These results point to the possibility of a two-step loading process whereby a pool of the CPC is loaded directly to inner centromere binding sites provided by pH3, and a second population of the complex is initially recruited to the kinetochore-proximal outer centromere by pH2A and subsequently translocated to the inner centromere. This proposed two-step process is somewhat similar to what has been suggested for Sgo1, which has been observed to first load to kinetochores in early mitosis, after which it relocalizes to inner centromeres to protect cohesion and in turn prevent premature sister chromatin separation (Liu et al., 2013, 2015; Hengeveld et al., 2017). Furthermore, a Sgo1 mutant unable to localize to kinetochores (Sgo1-K492A) cannot efficiently localize to centromeres (Liu et al., 2013, 2015), suggesting that Sgo1 must first bind kinetochores in order to eventually load onto centromeres (Liu et al., 2013, 2015; Hengeveld et al., 2017). This relocalization has been proposed to involve RNA polymerase II transcription and "opening" of dense centromeric chromatin (Liu et al., 2015). Finally, Sgo1 has been shown to delocalize from centromeres and relocalize to a region near CENP-C in Haspin knockout cells (Zhou et al., 2017), similar to what was observed for Borealin (Bekier et al., 2015) and Aurora B (Fig. 5, A and B) after Haspin inhibition. Based on these similarities, it is tempting to speculate that the CPC may be transported between different regions within the kinetochore and centromere, similar to what has been described for Sgo1. We note, however, that CPC "shuttling" is speculative, and that our data do not rule out other types of interdependencies between different CPC populations within the kinetochore and centromere.

Although the two distinct populations of the CPC recruited by histone phospho-modifications are required for efficient accumulation and activity of Aurora B at centromeres, our results suggest that neither modification is explicitly required for recruitment or activity of Aurora B at the outer kinetochore. Several studies corroborate this finding. (1) In chicken DT40 cells, a Survivin mutant lacking the centromere targeting domain is competent to rescue mitotic defects resulting from loss of inner centromere CPC after Survivin depletion (Yue et al., 2008). (2) In human cells, ectopic targeting of the CPC to centromeres does not restore Aurora B activity at kinetochores in cells that are depleted of Knl1, which prevents recruitment of phosphorylated, active Aurora B to kinetochores (Caldas et al., 2013). (3) In budding yeast, a mutation in Sli5/INCENP that disrupts CPC centromere localization, but not microtubule binding, has a minimal effect on chromosome bi-orientation and Aurora B–mediated error correction (Campbell and Desai, 2013). (4) Also in budding yeast, two groups have recently demonstrated that the CPC binds directly to the kinetochore COMA (Ctf19/Okp1/Mcm21/Ame1) complex (analogous to the human CENP-O/P/Q/U complex), and is recruited to kinetochores in cells. Importantly, this kinetochore-associated population is sufficient for Ipl1/Aurora kinase activity at kinetochores in the absence of centromere-localized CPC (Fischböck-Halwachs et al., 2019; García-Rodríguez et al., 2019). Together these results suggest that Aurora B activity at kinetochores can be uncoupled from centromere accumulation of the kinase. However, recent studies have also suggested that while centromere-localized Aurora B is not required per se for Aurora B phosphorylation of outer kinetochore substrates, it may be involved in properly regulating kinase activity in response to formation of stable kinetochore-microtubule attachments (Haase et al., 2017; Yoo et al., 2018). How inner centromere-localized Aurora B impacts this regulation remains to be resolved.

In agreement with our results, an accompanying paper from the Lens laboratory also demonstrated that Bub1 and Haspin are individually capable of recruiting the CPC to distinct locations within the kinetochore, and furthermore, they find that neither recruitment pathway is required for kinase activity of Aurora B at kinetochores (Hadders et al., 2020). Interestingly, in their study, CRISPR/Cas9-mediated Haspin knockout combined with Bub1 kinase inhibition resulted in impaired error correction as detected by a monastrol washout assay. In light of high Aurora B substrate phosphorylation at kinetochores under these conditions, this finding could be explained by a role for Haspin and/or Bub1 kinase activities in error correction separate from the kinetochore-associated Aurora B kinase–mediated mechanism (Zhou et al., 2017) or a role for centromere-localized Aurora B activity in error correction (e.g., mediated by phospho-MCAK; Andrews et al., 2004; Lan et al., 2004).

Several questions regarding the regulation of Aurora B localization remain to be addressed, including the following: What are the binding sites for kinetochore-localized Aurora B in metazoan cells? And how is kinase recruitment regulated such that Aurora B binds kinetochores with immature microtubule attachments but is evicted from those with mature, stable attachments? While these questions remain unresolved, our work suggests that there are at least two pathways for Aurora B recruitment to the kinetochore, one that requires Bub1 (but not its kinase activity) and one that does not. Previous work has demonstrated that localization and activity of kinetochore-associated Aurora B require the large kinetochore scaffolding protein Knl1 (Caldas et al., 2013), which directly recruits a complex of Bub1/Bub3 (Yamagishi et al., 2010; London et al., 2012; Shepperd et al., 2012; Primorac et al., 2013; Zhang et al., 2013; Vleugel et al., 2015). Thus, it is likely that the dependence of kinetochore-localized Aurora B on Knl1 is at least in part due to its recruitment of Bub1. Interestingly, we found in this study that in early mitosis, Aurora B binds to kinetochores at a location somewhere between CENP-C and the N terminus of Hec1 (Fig. 6). Of note, Knl1 resides in this vicinity of the kinetochore and has been suggested to undergo significant changes in conformation as kinetochores experience pulling forces from attached, dynamic microtubules (Wan et al., 2009; Roscioli et al., 2019). It is tempting to speculate that Knl1 and its

conformational changes upon kinetochore-microtubule stabilization may play a role in Aurora B kinase recruitment to and eviction from kinetochores, through both Bub1-dependent and Bub1-independent mechanisms. Further experiments are needed to explore this possibility.

Materials and methods

Cell culture and generation of cell lines

HeLa Kyoto cells were cultured in DMEM supplemented with 10% FBS, 1% antibiotic/antimycotic solution, and 4 mM L-glutamine and maintained at 37°C in 5% CO_2. U2OS osteosarcoma cells expressing an ectopic LacO array stably integrated into the short arm of chromosome 1 (a gift from S. Janicki, Wistar Institute, Philadelphia, PA; Janicki et al., 2004) were maintained in McCoy's 5A medium supplemented with 10% FBS and 1% antibiotic/antimycotic solution and maintained at 37°C in 5% CO_2. Flp-In T-REx HeLa host cells (a gift from S. Taylor, University of Manchester, England, UK) were cultured in DMEM supplemented with 10% FBS, 1% antibiotic/antimycotic solution, and 2 mM L-glutamine and maintained at 37°C in 5% CO_2. Stable cell lines expressing inducible WT-Sgo1-GFP, K492A-Sgo1-GFP, and T346A-Sgo1-GFP were generated from the Flp-In T-REx HeLa host cell line. Cells were grown to 50% confluency and transfected with 2.4 µg pOG44 recombinase-containing plasmid and 0.3 µg pcDNA5.FRT.TO-WT-, K492A-, or T346A- Sgo1-GFP plasmids with Fugene HD (Promega). The pcDNA5.FRT.TO-Sgo1 plasmids were generated through PCR amplification of WT Sgo1 (a gift from H. Yu, University of Texas Southwestern, Dallas, TX; Liu et al., 2013), and then cloned into a pcDNA5.FRT.TO vector through In-Fusion cloning. After 48 h, cells were switched to media containing 100 µg/ml hygromycin (EMD Millipore) and grown in selection media for 2 wk. Hygromycin-resistant foci were expanded and tested for inducible Sgo1-GFP expression. Cell lines expressing Sgo1 fusion proteins were cultured in DMEM supplemented with 10% FBS, 1% antibiotic/antimycotic solution, 2 mM L-glutamine, and 100 µg/ml hygromycin and maintained at 37°C in 5% CO_2. Gene expression was induced with 1 µg/ml doxycycline (Sigma-Aldrich) for 12–24 h.

Cell treatments and transfections

For live-cell imaging, cells were seeded and imaged in 35-mm glass-bottomed dishes (MatTek Corporation) and imaged in Leibovitz's L-15 medium (Invitrogen) supplemented with 10% FBS, 7 mM Hepes, and 4.5 g/liter glucose, pH 7.0. For fixed-cell analysis, cells were grown on sterile, acid-washed coverslips in six-well plates. U2OS cells were transfected with LacI-GFP, LacI-BFP, LacI-GFP-Bub1, LacI-BFP-Haspin, or LacI-GFP-Sgo1 vectors using Lipofectamine 2000 (Thermo Fisher Scientific). Transfection solutions were added to cells for 24 h, and then 9 µM RO-3306 (Sigma-Aldrich, Thermo Fisher Scientific) was added for an additional 20 h. Cells were then released from RO-3306 by washing with drug-free media for 30 min before fixation. For siRNA experiments, HeLa Kyoto cells were transfected with 8 µl of 20 µM stock siRNA solution using Oligofectamine (Thermo Fisher Scientific) and fixed 24 h after transfection. siRNA sequences are as follows: Sgo1: 5′-CAGTAGAACCTGCTCAGAAC C-3′ (Qiagen); Bub1: 5′-CAGCTTGTGATAAAGAGTCAA-3′ (Qiagen); and INCENP: 5′-CCGCATCATCTGTCACAGTTA-3′ (Qiagen). For Sgo1 overexpression experiments, Sgo1-GFP constructs were induced using 1 µg/ml doxycycline for 24 h. For Aurora B-GFP overexpression, HeLa Kyoto cells were transfected with a plasmid containing full-length human Aurora B fused to GFP using Lipofectamine 3000 (Thermo Fisher Scientific). For Haspin inhibition, cells were incubated with 10 µM 5-ITu (Sellechkchem) 30 min before fixation. For inhibition of Bub1 kinase, cells were treated with 10 µM BAY320 (provided by G. Siemeister, Bayer AG, Berlin, Germany) 30 min before fixation. For Aurora B kinase inhibition, cells were incubated with 20 µM ZM447439 (Tocris Biosciences) for 30 min before fixation. For monastrol washout experiments, HeLa Kyoto cells were synchronized in early mitosis using a double thymidine block and release. Briefly, cells were treated with 2.5 mM thymidine for 16 h, washed with PBS, replaced with fresh medium, and incubated for 8 h. For the second block, cells were again treated with 2.5 mM thymidine for 16 h. Cells were then washed with PBS and the medium replaced with fresh medium, and after 8 h, 150 µM monastrol (Tocris Biosciences) was added for 2 h. After 2 h, cells were washed with drug-free media and placed into either control media or media containing 10 µM ZM447439 or 10 µM BAY320 and imaged for 2 h.

Immunofluorescence

For U2OS LacO/LacI targeting and siRNA experiments, cells were rinsed in 37°C 60 mM PIPES, 25 mM HEPES, 10 mM EGTA, and 4 mM $MgSO_4$, pH 7.0 (PHEM buffer), and lysed at 37°C for 3 min in freshly prepared lysis buffer (PHEM buffer + 1% Triton X-100), followed by fixation for 20 min in 4% paraformaldehyde in PHEM buffer (37°C). After fixation, cells were washed 3 × 5 min in PHEM-T (PHEM buffer + 0.1% Triton X-100) and blocked in 10% boiled donkey serum (BDS) in PHEM for 1 h at room temperature. Primary antibodies were diluted in 5% BDS and added to coverslips overnight at 4°C. See Table 2 for primary antibody information. After primary antibody incubation, cells were rinsed 3 × 5 min in PHEM-T and then incubated for 45 min at RT with secondary antibodies conjugated to Alexa Fluor 488, Alexa Fluor 568, or Alexa Fluor 647 (Jackson ImmunoResearch Laboratories, Inc.) at 1:500 diluted in 5% BDS. Cells were rinsed 3 × 5 min in PHEM-T and quickly rinsed in PHEM followed by incubation in DAPI (2 ng/ml) diluted in PHEM for 30 s. Slides were rinsed 3 × 5 min in PHEM-T, quickly rinsed in PHEM, and then mounted onto glass slides with antifade solution (90% glycerol, 0.5% N-propyl gallate). Coverslips were sealed with nail polish and stored at 4°C. For two-color distance measurements and kinase inhibition experiments, cells were rinsed in 37°C PHEM buffer and permeabilized with a wash (30 s) in PHEM-T (0.5%) followed by fixation for 20 min in 4% paraformaldehyde in PHEM buffer (37°C). After fixation, cells were treated as described above. The double-affinity purified antibody against dual phosphorylated INCENP pS893 and pS894 was generated at 21st Century Biochemicals. For generation of the dual phospho-INCENP pS893, pS894 antibody, rabbits were immunized with a peptide corresponding to amino acids 887–901 of human INCENP phosphorylated at S893 and S894.

Table 2. **Details for all antibodies used in the study**

Antibody	Dilution	Source	Conditions
Immunofluorescence			
Mouse anti-pH3-T3	1:10,000	Gift, Dr. Hiroshi Kimura (Kelly et al., 2010)	1% TX 3 min, 4% PFA 20 min
Mouse anti-Sgo1	1:500	Abcam 58023	1% TX 3 min, 4% PFA 20 min
Rabbit anti-ABK	1:500	Abcam 2254	0.5% TX 30 s, 4% PFA 20 min; 1% TX 3 min, 4% PFA 20 min
Mouse anti-Bub1	1:200	Abcam 54893	0.5% TX 30 s, 4% PFA 20 min; 1% TX 3 min, 4% PFA 20 min
Rabbit anti-Bub1	1:200	Bethyl Laboratories A300-373A	1% TX 3 min, 4% PFA 20 min
Rabbit anti-pH2A-T120	1:1,000	Active Motif 39391	0.5% TX 30 s, 4% PFA 20 min; 1% TX 3 min, 4% PFA 20 min
Rabbit anti-pABK-T232	1:500	(DeLuca et al., 2017)	0.5% TX 30 s, 4% PFA 20 min; 1% TX 3 min, 4% PFA 20 min
Rabbit anti-pDsn1-S109	1:500	Gift, Dr. Iain Cheeseman (Welburn et al., 2010)	0.5% TX 30 s, 4% PFA 20 min
Rabbit anti-pHec1-S44	1:1,000	(DeLuca et al. 2011)	0.5% TX 30 s, 4% PFA 20 min; 1% TX 3 min, 4% PFA 20 min
Rabbit anti-pINCENP-S893,S894	1:400	This study	0.5% TX 30 s, 4% PFA 20 min
Rabbit anti-pKNL1-S24	1:400	Gift, Dr. Iain Cheeseman (Welburn et al., 2010)	0.5% TX 30 s, 4% PFA 20 min
Rabbit anti-Survivin	1:500	Santa Cruz Biotechnology 10811	1% TX 3 min, 4% PFA 20 min
Two-color distance measurements for centromere/kinetochore mapping			
Mouse anti-Hec1 (9G3)	1:2,000	GeneTex GTX70268	0.5% TX 30 s, 4% PFA 20 min
Guinea pig anti-CENP-C	1:500	MBL PD030	0.5% TX 30 s, 4% PFA 20 min
Rabbit anti-pH2A-T120	1:1,000	Active Motif 39391	0.5% TX 30 s, 4% PFA 20 min
Rabbit anti-pABK-T232	1:500	(DeLuca et al., 2017)	0.5% TX 30 s, 4% PFA 20 min
Western blotting			
Rabbit anti-pABK-T232	1:500	(DeLuca et al., 2017)	
Rabbit anti-pINCENP-S893,S894	1:500	This study	

For each antibody used for standard immunofluorescence experiments, two-color distance measurements, and Western blots, the table indicates the concentration used, antibody source, and fixation conditions. TX, Triton X-100; PFA, paraformaldehyde.

Imaging and data analysis

All fixed cell images were acquired on an IX71 inverted microscope (Olympus) incorporated into a DeltaVision Personal DV imaging system (GE Healthcare) using SoftWorx software (GE Healthcare). Slides were imaged using a 60× 1.42 NA differential interference contrast Plan Apochromat oil immersion lens (Olympus) and a CoolSNAP HQ2 camera. Images for two-color distance and fluorescence intensity measurements were acquired as z-stacks at 0.2-µm intervals. For two-color distance measurements, a 1.6 magnification lens was inserted in the light path, providing a final magnification of 67 nm/pixel at the camera sensor (CoolSNAP HQ2; Photometrics/Roper Technologies), and analysis was performed on kinetochore pairs that resided in a single focal plane from nondeconvolved images (with the exception of Aurora B–GFP images, which were deconvolved before analysis). The centroids of each kinetochore- or centromere-localized test antibody signal were determined in MATLAB (MathWorks) using SpeckleTracker, a customized program provided by X. Wan and T. Salmon (University of North Carolina, Chapel Hill, NC; Wan et al., 2009). Distances were then calculated using the identified centroids. Kinetochore (and in the case of pH2A-T120, kinetochore-proximal outer centromere) fluorescence intensities of pABK-T232, pHec1-S44, pKnl1-S24, and pH2A-T120 were quantified from images in MATLAB using the customized SpeckleTracker program. Centromere fluorescence intensities were measured using MetaMorph software (Molecular Devices) by centering a 9-pixel-diameter circle between two sister kinetochores, placing two additional 9-pixel circles adjacent to the first circle, and logging the total integrated intensities. For each centromere measurement, the average background fluorescence intensity was calculated by averaging the two adjacent circles and subtracting this value from the integrated intensity logged from the centromere circle. Whole cell intensity values were calculated by first generating maximum intensity projections from nondeconvolved z-stacks. A large, 150-pixel-diameter circle was placed around the cell, and total fluorescence intensity was logged. In addition, six 15-pixel-diameter circles were placed outside the large circle, and fluorescence intensities were logged. The background intensity was determined by averaging the fluorescence intensity values from the six smaller circles, calculating the per-pixel intensity value, and multiplying by the area of the large circle. Finally, the background-corrected whole cell intensity was calculated by subtracting the background value from the total integrated intensity of the large circle. For quantification of LacO/LacI experiments, recruitment of CPC components to the LacO array was determined by measuring fluorescence intensity within the LacI-positive

region using maximum intensity projected images with FIJI software. Background values were determined by measuring the average intensity of each test antibody at the LacI-GFP or LacI-BFP ectopic locus (measured in cells expressing LacI-GFP or LacI-BFP only, not fused to a test protein). In each experiment using a targeted LacI-fusion protein, cells were considered "positive" if the fluorescence intensity at the locus was higher than the average background values. For live cell experiments, images were collected on a Nikon Ti-E microscope equipped with a Plan apochromatic, differential interference contrast, 0.95 NA 40× total internal reflection fluorescence objective, a Ti-S-E motorized stage, piezo Z-control (Physik Instruments), a spinning disc confocal scanner unit (CSUX1; Yokogawa), and an iXon DU888 cooled EM-CCD camera (Andor). Cells were imaged every 5 min for 2 h; 3 × 1 µm z-sections were taken at each time point. All statistical analyses were performed in Prism software (GraphPad).

In vitro phosphatase assay

A complex of Aurora B kinase (amino acids 60–361) and INCENP (amino acids 1–68 and 834–900) was generated by expressing the constructs in BL21DE3 cells by induction with IPTG overnight at 18°. Cells were lysed by sonication and centrifuged at 45,000 rpm. The supernatant fraction was purified on glutathione resin (Pierce 16100), followed by cleavage of the GST moiety with HRV-3C protease. For the phosphatase assay, 1.7 µM Aurora B/INCENP complex was incubated with or without lambda protein phosphatase (2,400 U; NEB P0753S) in 1× NEBuffer for protein metallophosphatases and 1 mM $MnCl_2$, for 30 min at 30°C. Reactions were terminated with the addition of 5× SDS-PAGE sample buffer. Samples for pABK-T232 and pINCENP-S893, S894 were run on 12% and 15% SDS-polyacrylamide gels, respectively, transferred to polyvinylidene difluoride membrane (GE 10600030), and processed for Western blotting. For phospho-staining, blots were incubated with pABK-T232 and pINCENP-S893, S894 at 1:500 (1% BSA in TBS). Primary antibodies (see Table 1 for details) were detected using horseradish peroxidase–conjugated anti-rabbit secondary antibody at 1:10,000 (Jackson ImmunoResearch Laboratories, Inc.) and enhanced chemiluminescence. Reactions with and without lambda phosphatase were run on 15% SDS-polyacrylamide gels and stained with Coomassie brilliant blue for total protein.

Online supplemental material

Fig. S1 shows that Sgo1-LacI is sufficient to recruit Aurora B to an ectopic chromosome locus in U2OS cells independent of Bub1 and pH2A-T120, and that Bub1-LacI requires Sgo1 to recruit Aurora B to an ectopic locus in U2OS cells. Fig. S2 demonstrates that depletion of Bub1 protein results in a reduction of both centromere and kinetochore-associated Aurora B kinase in human cells. Fig. S3 shows the characterization of an anti-pINCENP-S893, S894 antibody through colocalization with Aurora B at various mitotic phases in HeLa cells and treatment with ZM447439 (an Aurora B inhibitor), INCENP siRNA, and lambda phosphatase. Fig. S4 shows the specificity of the Bub1 and Haspin kinase inhibitors BAY320 and 5-ITu. Fig. S5 demonstrates that Haspin inhibition prevents accumulation and activity of Aurora B kinase at centromeres, but not at kinetochores.

Acknowledgments

The authors thank Drs. Hongtao Yu (University of Texas Southwestern, Dallas, TX), Hiroshi Kimura (Tokyo Institute of Technology, Tokyo, Japan), Stephen Taylor (University of Manchester, Manchester, UK), Gerhard Siemeister (Bayer AG, Berlin, Germany), Iain Cheeseman (Massachusetts Institute of Technology, Cambridge, MA), Ted Salmon (University of North Carolina, Chapel Hill, NC), Xiaohu Wan (University of North Carolina, Chapel Hill, NC), and Susan Janicki (Wistar Institute, Philadelphia, PA) for generous sharing of reagents and tools, Jeanne Mick for technical contributions, and Drs. Mekonnen Lemma Dechassa and Karolin Luger for their help and insight on the project.

This work was suported by grants from the National Institutes of Health, National Institute of General Medical Sciences, to J.G. DeLuca (R01-GM088371 and R35-GM130365).

The authors declare no competing financial interests.

Author contributions: A.J. Broad, K.F. DeLuca, and J.G. DeLuca conceived the project, and J.G. DeLuca supervised the project. A.J. Broad and K.F. DeLuca carried out the experiments and analyzed the data. J.G. DeLuca helped with data analysis. A.J. Broad and J.G. DeLuca wrote the paper with input from K.F. DeLuca.

Submitted: 17 May 2019
Revised: 26 November 2019
Accepted: 8 January 2020

References

Akiyoshi, B., C.R. Nelson, and S. Biggins. 2013. The aurora B kinase promotes inner and outer kinetochore interactions in budding yeast. *Genetics*. 194: 785–789. https://doi.org/10.1534/genetics.113.150839

Andrews, P.D., Y. Ovechkina, N. Morrice, M. Wagenbach, K. Duncan, L. Wordeman, and J.R. Swedlow. 2004. Aurora B regulates MCAK at the mitotic centromere. *Dev. Cell.* 6:253–268. https://doi.org/10.1016/S1534-5807(04)00025-5

Bakhoum, S.F., S.L. Thompson, A.L. Manning, and D.A. Compton. 2009. Genome stability is ensured by temporal control of kinetochore-microtubule dynamics. *Nat. Cell Biol.* 11:27–35. https://doi.org/10.1038/ncb1809

Baron, A.P., C. von Schubert, F. Cubizolles, G. Siemeister, M. Hitchcock, A. Mengel, J. Schröder, A. Fernández-Montalván, F. von Nussbaum, D. Mumberg, and E.A. Nigg. 2016. Probing the catalytic functions of Bub1 kinase using the small molecule inhibitors BAY-320 and BAY-524. *eLife*. 5:e12187. https://doi.org/10.7554/eLife.12187

Bekier, M.E., T. Mazur, M.S. Rashid, and W.R. Taylor. 2015. Borealin dimerization mediates optimal CPC checkpoint function by enhancing localization to centromeres and kinetochores. *Nat. Commun.* 6:6775. https://doi.org/10.1038/ncomms7775

Biggins, S., F.F. Severin, N. Bhalla, I. Sassoon, A.A. Hyman, and A.W. Murray. 1999. The conserved protein kinase Ipl1 regulates microtubule binding to kinetochores in budding yeast. *Genes Dev.* 13:532–544. https://doi.org/10.1101/gad.13.5.532

Bishop, J.D., and J.M. Schumacher. 2002. Phosphorylation of the carboxyl terminus of inner centromere protein (INCENP) by the Aurora B Kinase stimulates Aurora B kinase activity. *J. Biol. Chem.* 277:27577–27580. https://doi.org/10.1074/jbc.C200307200

Caldas, G.V., K.F. DeLuca, and J.G. DeLuca. 2013. KNL1 facilitates phosphorylation of outer kinetochore proteins by promoting Aurora B kinase activity. *J. Cell Biol.* 203:957–969. https://doi.org/10.1083/jcb.201306054

Campbell, C.S., and A. Desai. 2013. Tension sensing by Aurora B kinase is independent of survivin-based centromere localization. *Nature*. 497: 118–121. https://doi.org/10.1038/nature12057

Carmena, M., M. Wheelock, H. Funabiki, and W.C. Earnshaw. 2012. The chromosomal passenger complex (CPC): from easy rider to the

godfather of mitosis. *Nat. Rev. Mol. Cell Biol.* 13:789–803. https://doi.org/10.1038/nrm3474

Cheeseman, I.M., J.S. Chappie, E.M. Wilson-Kubalek, and A. Desai. 2006. The conserved KMN network constitutes the core microtubule-binding site of the kinetochore. *Cell.* 127:983–997. https://doi.org/10.1016/j.cell.2006.09.039

Cimini, D., X. Wan, C.B. Hirel, and E.D. Salmon. 2006. Aurora kinase promotes turnover of kinetochore microtubules to reduce chromosome segregation errors. *Curr. Biol.* 16:1711–1718. https://doi.org/10.1016/j.cub.2006.07.022

De Antoni, A., S. Maffini, S. Knapp, A. Musacchio, and S. Santaguida. 2012. A small-molecule inhibitor of Haspin alters the kinetochore functions of Aurora B. *J. Cell Biol.* 199:269–284. https://doi.org/10.1083/jcb.201205119

DeLuca, J.G., W.E. Gall, C. Ciferri, D. Cimini, A. Musacchio, and E.D. Salmon. 2006. Kinetochore microtubule dynamics and attachment stability are regulated by Hec1. *Cell.* 127:969–982. https://doi.org/10.1016/j.cell.2006.09.047

DeLuca, K.F., S.M.A. Lens, and J.G. DeLuca. 2011. Temporal changes in Hec1 phosphorylation control kinetochore-microtubule attachment stability during mitosis. *J. Cell Sci.* 124:622–634. https://doi.org/10.1242/jcs.072629

DeLuca, K.F., A. Meppelink, A.J. Broad, J.E. Mick, O.B. Peersen, S. Pektas, S.M.A. Lens, and J.G. DeLuca. 2017. Aurora A kinase phosphorylates Hec1 to regulate metaphase kinetochore–microtubule dynamics. *The Journal of Cell Biology*. 217(1):163–177.

Ditchfield, C., V.L. Johnson, A. Tighe, R. Ellston, C. Haworth, T. Johnson, A. Mortlock, N. Keen, and S.S. Taylor. 2003. Aurora B couples chromosome alignment with anaphase by targeting BubR1, Mad2, and Cenp-E to kinetochores. *J. Cell Biol.* 161:267–280. https://doi.org/10.1083/jcb.200208091

Etemad, B., and G.J. Kops. 2016. Attachment issues: kinetochore transformations and spindle checkpoint silencing. *Curr. Opin. Cell Biol.* 39:101–108. https://doi.org/10.1016/j.ceb.2016.02.016

Etemad, B., T.E. Kuijt, and G.J. Kops. 2015. Kinetochore-microtubule attachment is sufficient to satisfy the human spindle assembly checkpoint. *Nat. Commun.* 6:8987. https://doi.org/10.1038/ncomms9987

Fischböck-Halwachs, J., S. Singh, M. Potocnjak, G. Hagemann, V. Solis-Mezarino, S. Woike, M. Ghodgaonkar-Steger, F. Weissmann, L.D. Gallego, J. Rojas, et al. 2019. The COMA complex interacts with Cse4 and positions Sli15/Ipl1 at the budding yeast inner kinetochore. *eLife.* 8:e42879. https://doi.org/10.7554/eLife.42879

García-Rodríguez, L.J., T. Kasciukovic, V. Denninger, and T.U. Tanaka. 2019. Aurora B-INCENP Localization at Centromeres/Inner Kinetochores Is Required for Chromosome Bi-orientation in Budding Yeast. *Curr. Biol.* 29:1536–1544.e4. https://doi.org/10.1016/j.cub.2019.03.051

Godek, K.M., L. Kabeche, and D.A. Compton. 2015. Regulation of kinetochore-microtubule attachments through homeostatic control during mitosis. *Nat. Rev. Mol. Cell Biol.* 16:57–64. https://doi.org/10.1038/nrm3916

Haase, J., M.K. Bonner, H. Halas, and A.E. Kelly. 2017. Distinct roles of the chromosomal passenger complex in the detection of and response to errors in kinetochore-microtubule attachment. *Dev. Cell.* 42:640–654.e5. https://doi.org/10.1016/j.devcel.2017.08.022

Hadders, M.A., S. Hindriksen, M.A. Truong, A.N. Mhaskar, J.P. Wopkem, M.J.M. Vromans, and S.M.A. Lens. 2020. Untangling the contribution of Haspin and Bub1 to Aurora B function during mitosis. *J. Cell Biol.* https://doi.org/10.1083/jcb.201907087

Hara, M., M. Ariyoshi, E.-I. Okumura, T. Hori, and T. Fukagawa. 2018. Multiple phosphorylations control recruitment of the KMN network onto kinetochores. *Nat. Cell Biol.* 20:1378–1388. https://doi.org/10.1038/s41556-018-0230-0

Hengeveld, R.C.C., M.J.M. Vromans, M. Vleugel, M.A. Hadders, and S.M.A. Lens. 2017. Inner centromere localization of the CPC maintains centromere cohesion and allows mitotic checkpoint silencing. *Nat. Commun.* 8:15542. https://doi.org/10.1038/ncomms15542

Hindriksen, S., S.M.A. Lens, and M.A. Hadders. 2017. The ins and outs of Aurora B inner centromere localization. *Front. Cell Dev. Biol.* 5:112. https://doi.org/10.3389/fcell.2017.00112

Janicki, S.M., T. Tsukamoto, S.E. Salghetti, W.P. Tansey, R. Sachidanandam, K.V. Prasanth, T. Ried, Y. Shav-Tal, E. Bertrand, R.H. Singer, and D.L. Spector. 2004. From silencing to gene expression: real-time analysis in single cells. *Cell.* 116:683–698. https://doi.org/10.1016/S0092-8674(04)00171-0

Kapoor, T.M., T.U. Mayer, M.L. Coughlin, and T.J. Mitchison. 2000. Probing spindle assembly mechanisms with monastrol, a small molecule inhibitor of the mitotic kinesin, Eg5. *J. Cell Biol.* 150:975–988. https://doi.org/10.1083/jcb.150.5.975

Kawashima, S.A., T. Tsukahara, M. Langegger, S. Hauf, T.S. Kitajima, and Y. Watanabe. 2007. Shugoshin enables tension-generating attachment of kinetochores by loading Aurora to centromeres. *Genes Dev.* 21:420–435. https://doi.org/10.1101/gad.1497307

Kawashima, S.A., Y. Yamagishi, T. Honda, K. Ishiguro, and Y. Watanabe. 2010. Phosphorylation of H2A by Bub1 prevents chromosomal instability through localizing shugoshin. *Science.* 327:172–177. https://doi.org/10.1126/science.1180189

Kelly, A.E., C. Ghenoiu, J.Z. Xue, C. Zierhut, H. Kimura, and H. Funabiki. 2010. Survivin reads phosphorylated histone H3 threonine 3 to activate the mitotic kinase Aurora B. *Science.* 330:235–239. https://doi.org/10.1126/science.1189505

Kim, S., and H. Yu. 2015. Multiple assembly mechanisms anchor the KMN spindle checkpoint platform at human mitotic kinetochores. *J. Cell Biol.* 208:181–196. https://doi.org/10.1083/jcb.201407074

Krenn, V., and A. Musacchio. 2015. The Aurora B kinase in chromosome bi-orientation and spindle checkpoint signaling. *Front. Oncol.* 5:225. https://doi.org/10.3389/fonc.2015.00225

Lampson, M.A., and I.M. Cheeseman. 2011. Sensing centromere tension: Aurora B and the regulation of kinetochore function. *Trends Cell Biol.* 21:133–140. https://doi.org/10.1016/j.tcb.2010.10.007

Lampson, M.A., and T.M. Kapoor. 2005. The human mitotic checkpoint protein BubR1 regulates chromosome-spindle attachments. *Nat. Cell Biol.* 7:93–98. https://doi.org/10.1038/ncb1208

Lan, W., X. Zhang, S.L. Kline-Smith, S.E. Rosasco, G.A. Barrett-Wilt, J. Shabanowitz, D.F. Hunt, C.E. Walczak, and P.T. Stukenberg. 2004. Aurora B phosphorylates centromeric MCAK and regulates its localization and microtubule depolymerization activity. *Curr. Biol.* 14:273–286. https://doi.org/10.1016/j.cub.2004.01.055

Liu, D., G. Vader, M.J. Vromans, M.A. Lampson, and S.M.A. Lens. 2009. Sensing chromosome bi-orientation by spatial separation of aurora B kinase from kinetochore substrates. *Science.* 323:1350–1353. https://doi.org/10.1126/science.1167000

Liu, H., L. Jia, and H. Yu. 2013. Phospho-H2A and cohesin specify distinct tension-regulated Sgo1 pools at kinetochores and inner centromeres. *Curr. Biol.* 23:1927–1933. https://doi.org/10.1016/j.cub.2013.07.078

Liu, H., Q. Qu, R. Warrington, A. Rice, N. Cheng, and H. Yu. 2015. Mitotic transcription installs Sgo1 at centromeres to coordinate chromosome segregation. *Mol. Cell.* 59:426–436. https://doi.org/10.1016/j.molcel.2015.06.018

London, N., S. Ceto, J.A. Ranish, and S. Biggins. 2012. Phosphoregulation of Spc105 by Mps1 and PP1 Regulates Bub1 Localization to Kinetochores. *Current Biology*. 22(10):900–906.

Maresca, T.J., and E.D. Salmon. 2009. Intrakinetochore stretch is associated with changes in kinetochore phosphorylation and spindle assembly checkpoint activity. *J. Cell Biol.* 184:373–381. https://doi.org/10.1083/jcb.200808130

Meppelink, A., L. Kabeche, M.J.M. Vromans, D.A. Compton, and S.M.A. Lens. 2015. Shugoshin-1 balances Aurora B kinase activity via PP2A to promote chromosome bi-orientation. *Cell Reports.* 11:508–515. https://doi.org/10.1016/j.celrep.2015.03.052

Musacchio, A., and A. Desai. 2017. A molecular view of kinetochore assembly and function. *Biology (Basel).* 6:1.

Posch, M., G.A. Khoudoli, S. Swift, E.M. King, J.G. Deluca, and J.R. Swedlow. 2010. Sds22 regulates aurora B activity and microtubule-kinetochore interactions at mitosis. *J. Cell Biol.* 191:61–74. https://doi.org/10.1083/jcb.200912046

Primorac, I., J.R. Weir, E. Chiroli, F. Gross, I. Hoffmann, S. van Gerwen, A. Ciliberto, and A. Musacchio. 2013. Bub3 reads phosphorylated MELT repeats to promote spindle assembly checkpoint signaling. *eLife.* 2.

Rago, F., K.E. Gascoigne, and I.M. Cheeseman. 2015. Distinct organization and regulation of the outer kinetochore KMN network downstream of CENP-C and CENP-T. *Curr. Biol.* 25:671–677. https://doi.org/10.1016/j.cub.2015.01.059

Ricke, R.M., K.B. Jeganathan, and J.M. van Deursen. 2011. Bub1 overexpression induces aneuploidy and tumor formation through Aurora B kinase hyperactivation. *J. Cell Biol.* 193:1049–1064. https://doi.org/10.1083/jcb.201012035

Ricke, R.M., K.B. Jeganathan, L. Malureanu, A.M. Harrison, and J.M. van Deursen. 2012. Bub1 kinase activity drives error correction and mitotic checkpoint control but not tumor suppression. *J. Cell Biol.* 199:931–949. https://doi.org/10.1083/jcb.201205115

Roscioli, E., T.E. Germanova, C.A. Smith, P.A. Embacher, M. Erent, A.I. Thompson, N.J. Burroughs, and A.D. McAnish. 2019. Ensemble- level organization of human kinetochores and evidence for distinct tension and attachment sensors. bioRxiv. doi: https://doi.org/10.1101/685248 (Preprint posted June 28, 2019)

Salimian, K.J., E.R. Ballister, E.M. Smoak, S. Wood, T. Panchenko, M.A. Lampson, and B.E. Black. 2011. Feedback control in sensing chromosome biorientation by the Aurora B kinase. *Curr. Biol.* 21:1158–1165. https://doi.org/10.1016/j.cub.2011.06.015

Salmon, E.D., D. Cimini, L.A. Cameron, and J.G. DeLuca. 2005. Merotelic kinetochores in mammalian tissue cells. *Philos. Trans. R. Soc. Lond. B Biol. Sci.* 360:553–568. https://doi.org/10.1098/rstb.2004.1610

Sessa, F., M. Mapelli, C. Ciferri, C. Tarricone, L.B. Areces, T.R. Schneider, P.T. Stukenberg, and A. Musacchio. 2005. Mechanism of Aurora B activation by INCENP and inhibition by hesperadin. *Mol. Cell.* 18:379–391. https://doi.org/10.1016/j.molcel.2005.03.031

Shepperd, L.A., J.C. Meadows, A.M. Sochaj, T.C. Lancaster, J. Zou, G.J. Buttrick, J. Rappsilber, K.G. Hardwick, and J.B.A. Millar. 2012. Phosphodependent Recruitment of Bub1 and Bub3 to Spc7/KNL1 by Mph1 Kinase Maintains the Spindle Checkpoint. *Current Biology*. 22(10):891–899.

Suzuki, A., S.K. Long, and E.D. Salmon. 2018. An optimized method for 3D fluorescence co-localization applied to human kinetochore protein architecture. *eLife.* 7:e32418. https://doi.org/10.7554/eLife.32418

Tanaka, T.U., N. Rachidi, C. Janke, G. Pereira, M. Galova, E. Schiebel, M.J.R. Stark, and K. Nasmyth. 2002. Evidence that the Ipl1-Sli15 (Aurora kinase-INCENP) complex promotes chromosome bi-orientation by altering kinetochore-spindle pole connections. *Cell.* 108:317–329. https://doi.org/10.1016/S0092-8674(02)00633-5

Tauchman, E.C., F.J. Boehm, and J.G. DeLuca. 2015. Stable kinetochore-microtubule attachment is sufficient to silence the spindle assembly checkpoint in human cells. *Nat. Commun.* 6:10036. https://doi.org/10.1038/ncomms10036

Trivedi, P., A.V. Zaytsev, M. Godzi, F.I. Ataullakhanov, E.L. Grishchuk, and P.T. Stukenberg. 2019. The binding of Borealin to microtubules underlies a tension independent kinetochore-microtubule error correction pathway. *Nat Commun.* 10(1).

Tsukahara, T., Y. Tanno, and Y. Watanabe. 2010. Phosphorylation of the CPC by Cdk1 promotes chromosome bi-orientation. *Nature.* 467:719–723. https://doi.org/10.1038/nature09390

Uchida, K.S.K., K. Takagaki, K. Kumada, Y. Hirayama, T. Noda, and T. Hirota. 2009. Kinetochore stretching inactivates the spindle assembly checkpoint. *J. Cell Biol.* 184:383–390. https://doi.org/10.1083/jcb.200811028

van der Horst, A., and S.M.A. Lens. 2014. Cell division: control of the chromosomal passenger complex in time and space. *Chromosoma.* 123:25–42. https://doi.org/10.1007/s00412-013-0437-6

Vleugel, M., M. Omerzu, V. Groenewold, M.A. Hadders, S.M.A. Lens, and G.J.P.L. Kops. 2015. Sequential Multisite Phospho-Regulation of KNL1-BUB3 Interfaces at Mitotic Kinetochores. *Molecular Cell*. 57(5): 824–835.

Wan, X., R.P. O'Quinn, H.L. Pierce, A.P. Joglekar, W.E. Gall, J.G. DeLuca, C.W. Carroll, S.T. Liu, T.J. Yen, B.F. McEwen, et al. 2009. Protein architecture of the human kinetochore microtubule attachment site. *Cell.* 137: 672–684. https://doi.org/10.1016/j.cell.2009.03.035

Wang, F., J. Dai, J.R. Daum, E. Niedzialkowska, B. Benerjee, P.T. Stukenberg, G.J. Gorbsky, and J.M. Higgins. 2010. Histone H3 Thr-3 phosphorylation at centromeres in mitosis. *Science.* 330:231–235. https://doi.org/10.1126/science.1189435

Wang, F., N.P. Ulyanova, J.R. Daum, D. Patnaik, A.V. Kateneva, G.J. Gorbsky, and J.M. Higgins. 2012. Haspin inhibitors reveal centromeric functions of Aurora B in chromosome segregation. *J. Cell Biol.* 199:251–268. https://doi.org/10.1083/jcb.201205106

Watanabe, Y. 2010. Temporal and spatial regulation of targeting aurora B to the inner centromere. *Cold Spring Harb. Symp. Quant. Biol.* 75:419–423. https://doi.org/10.1101/sqb.2010.75.035

Welburn, J.P.I., M. Vleugel, D. Liu, J.R. Yates III, M.A. Lampson, T. Fukagawa, and I.M. Cheeseman. 2010. Aurora B phosphorylates spatially distinct targets to differentially regulate the kinetochore-microtubule interface. *Mol. Cell.* 38:383–392. https://doi.org/10.1016/j.molcel.2010.02.034

Yamagishi, Y., T. Honda, Y. Tanno, and Y. Watanabe. 2010. Two histone marks establish the inner centromere and chromosome bi-orientation. *Science.* 330:239–243. https://doi.org/10.1126/science.1194498

Yoo, T.Y., J.M. Choi, W. Conway, C.H. Yu, R.V. Pappu, and D.J. Needleman. 2018. Measuring NDC80 binding reveals the molecular basis of tension-dependent kinetochore-microtubule attachments. *eLife.* 7:e36392. https://doi.org/10.7554/eLife.36392

Yue, Z., A. Carvalho, Z. Xu, X. Yuan, S. Cardinale, S. Ribeiro, F. Lai, H. Ogawa, E. Gudmundsdottir, R. Gassmann, et al. 2008. Deconstructing Survivin: comprehensive genetic analysis of Survivin function by conditional knockout in a vertebrate cell line. *J. Cell Biol.* 183:279–296. https://doi.org/10.1083/jcb.200806118

Zaytsev, A.V., and E.L. Grishchuk. 2015. Basic mechanism for biorientation of mitotic chromosomes is provided by the kinetochore geometry and indiscriminate turnover of kinetochore microtubules. *Mol. Biol. Cell.* 26: 3985–3998. https://doi.org/10.1091/mbc.E15-06-0384

Zaytsev, A.V., L.J.R. Sundin, K.F. DeLuca, E.L. Grishchuk, and J.G. DeLuca. 2014. Accurate phosphoregulation of kinetochore-microtubule affinity requires unconstrained molecular interactions. *J. Cell Biol.* 206:45–59. https://doi.org/10.1083/jcb.201312107

Zhai, Y., P.J. Kronebusch, and G.G. Borisy. 1995. Kinetochore microtubule dynamics and the metaphase-anaphase transition. *J. Cell Biol.* 131: 721–734. https://doi.org/10.1083/jcb.131.3.721

Zhang, G., T. Lischetti, and J. Nilsson. 2013. A minimal number of MELT repeats supports all the functions of KNL1 in chromosome segregation. *J Cell Sci.* 127(4):871–884.

Zhou, L., C. Liang, Q. Chen, Z. Zhang, B. Zhang, H. Yan, F. Qi, M. Zhang, Q. Yi, Y. Guan, et al. 2017. The N-Terminal non-kinase-domain-mediated binding of Haspin to Pds5B protects centromeric cohesion in mitosis. *Curr. Biol.* 27:992–1004. https://doi.org/10.1016/j.cub.2017.02.019

Supplemental material

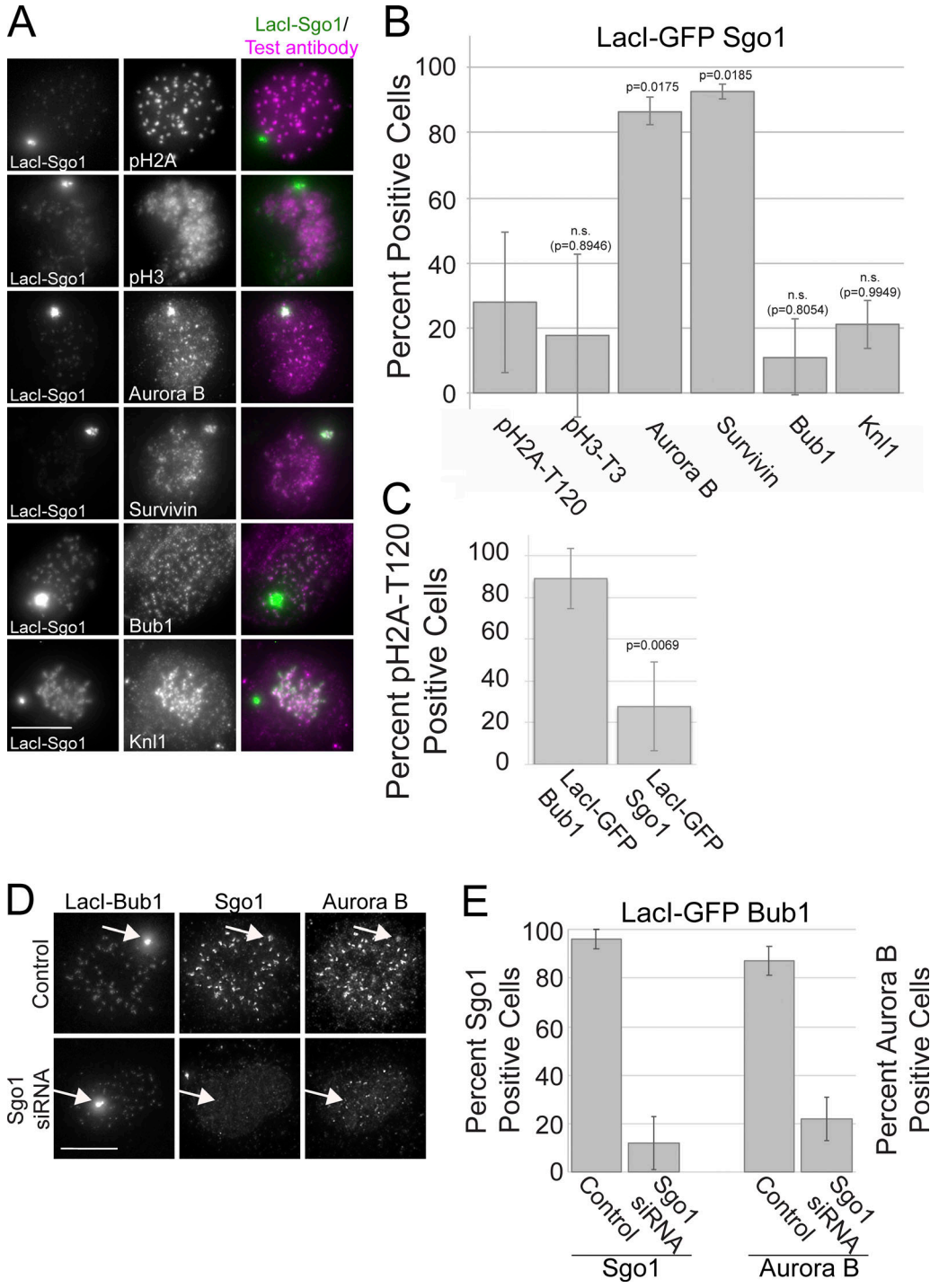

Figure S1. **Sgo1 recruits the CPC to an ectopic chromosome locus in human cells. (A)** Immunofluorescence images of U2OS cells expressing LacI-GFP-Sgo1. Cells were immunostained for the indicated proteins or phospho-histone epitopes and analyzed for positive recruitment based on a threshold intensity determined from U2OS cells expressing LacI-GFP. **(B)** Quantification of the recruitment of indicated proteins or phospho-epitopes in LacI-GFP-Sgo1–expressing cells. **(C)** Quantification of pH2A-T120 recruitment in Bub1 or Sgo1-LacI–expressing cells. For all conditions, cells were synchronized in G2 using RO-3306 and washed out of drug 30 min before fixation to enrich for mitotic cells. **(D)** Immunofluorescence images of U2OS cells expressing LacI-GFP-Bub1. Top row: control; bottom row: Sgo1 siRNA. **(E)** Quantification of percent Sgo1-positive cells (left) and percent Aurora B–positive cells (right) in control and Sgo1 siRNA-treated cells. For each condition shown, ≥20 cells were quantified from at least two independent experiments. Error bars represent SD. For B, significance values were calculated using a one-way ordinary ANOVA test. Shown are significance values between experiments for each test antibody and pH2A-T120. For C, the significance value was calculated using an unpaired nonparametric Student's *t* test. Scale bars, 10 µm.

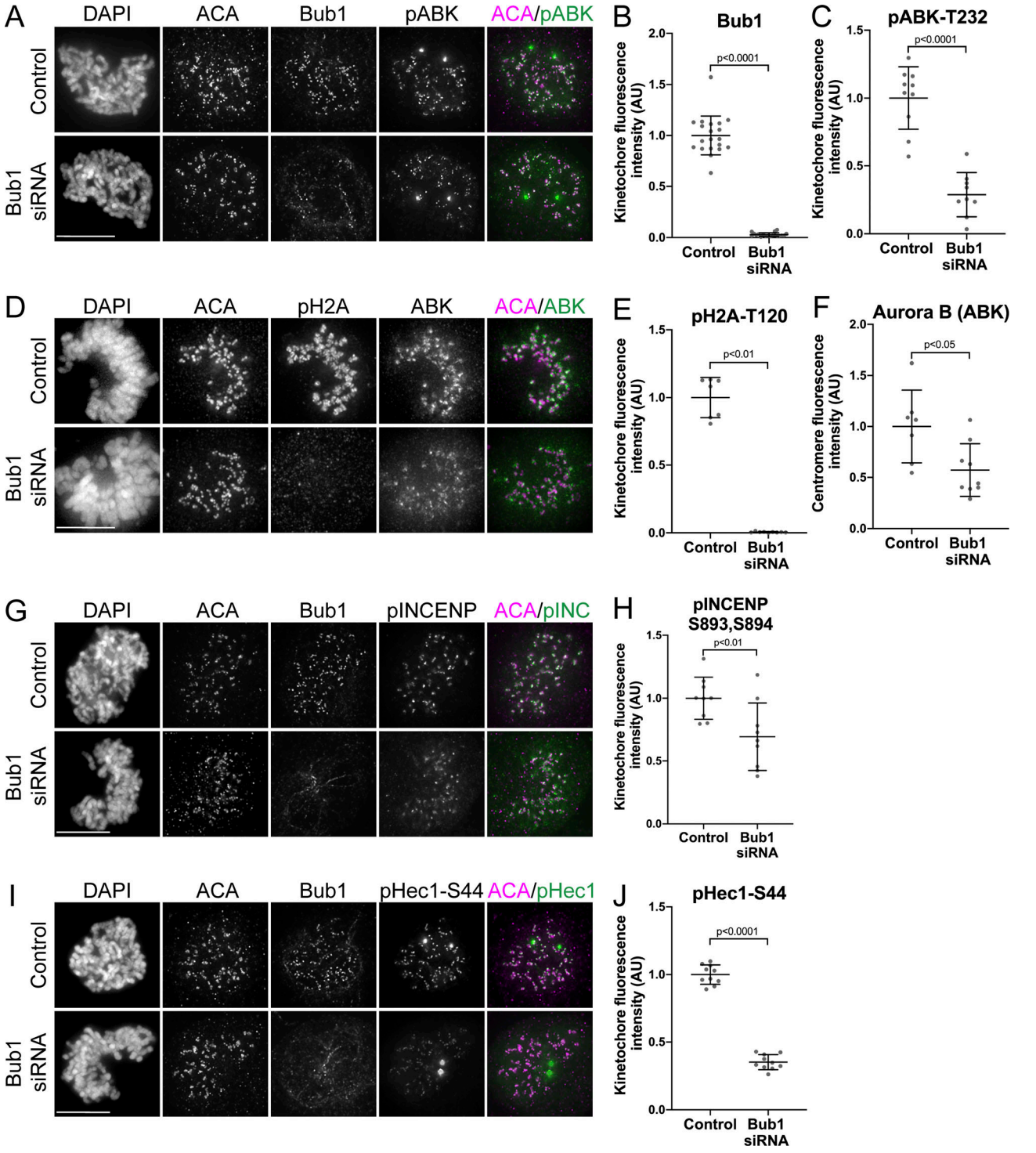

Figure S2. **Depletion of Bub1 protein results in reduction of both centromere and kinetochore-associated Aurora B in human cells. (A, D, G, and I)** Immunofluorescence images of HeLa cells depleted of Bub1 and immunostained for the indicated antibodies. **(B, C, E, F, H, and J)** Quantification of kinetochore or centromere fluorescence intensities of indicated antibodies. Error bars indicate SD. For all conditions, at least 120 kinetochores from 10 cells were measured from a total of three independent experiments. Error bars represent SD. Significance values were calculated using unpaired nonparametric Student's *t* tests. Scale bars, 10 µm. AU, arbitrary units.

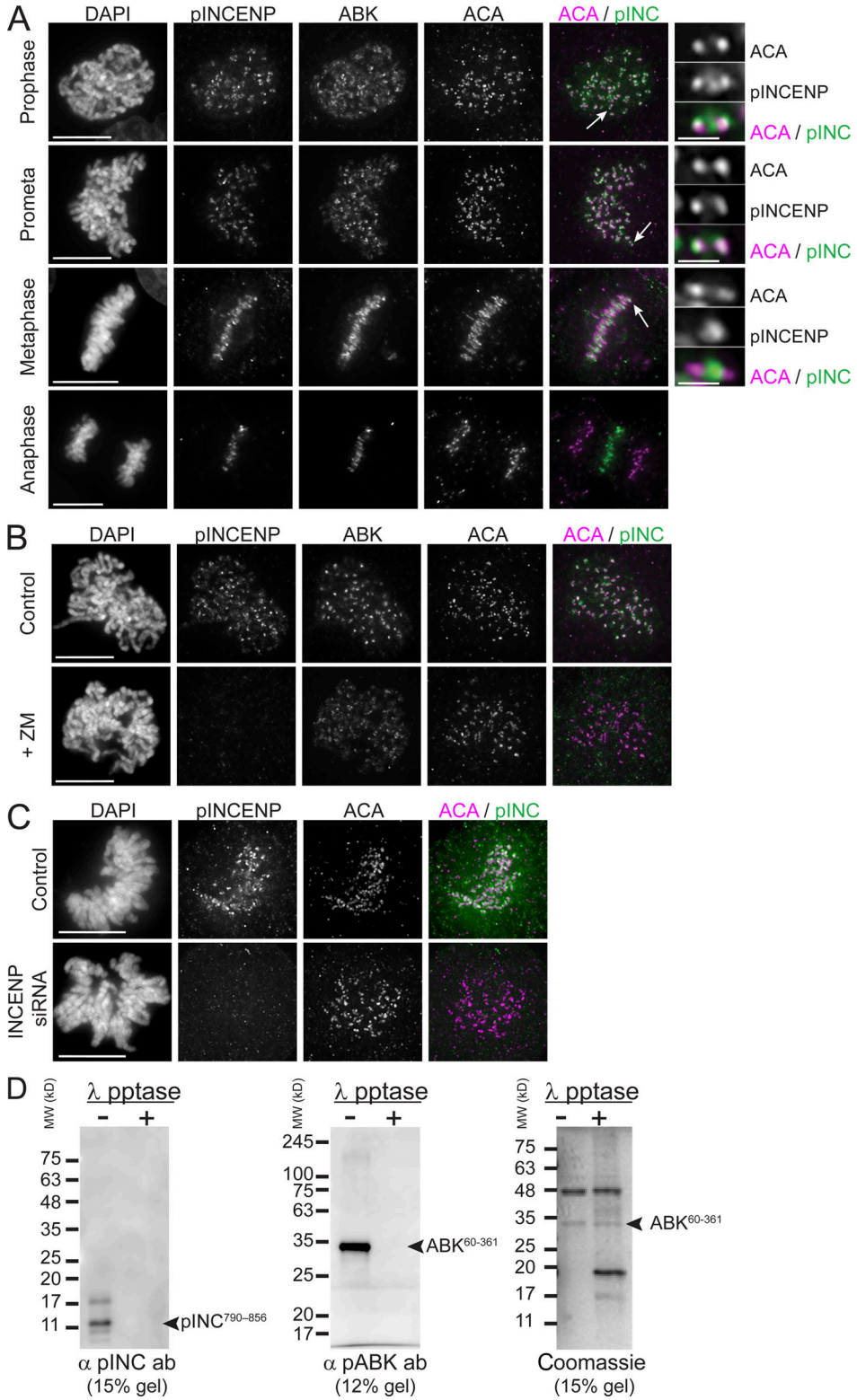

Figure S3. **Characterization of pINCENP-S893,894 antibody. (A)** Immunofluorescence images of HeLa cells in various stages of mitosis stained with pINCENP-S893, S894, Aurora B, and ACA. Arrows point to the kinetochore pairs shown in the insets on the right. **(B)** Immunofluorescence images of a control HeLa cell and a HeLa cell treated with 10 µM ZM447439. **(C)** Immunofluorescence images of a control cell and HeLa cell treated with INCENP siRNA. **(D)** A complex of Aurora B (amino acids 60–361) and INCENP (amino acids 1–68 and 834–900) was incubated with or without lambda protein phosphatase (pptase), and reactions were terminated with the addition of SDS-PAGE sample buffer. Images show Western blots of reactions probed with pINCENP-S893, S894 (left) and pABK-T232 (middle) antibodies (ab). A Coomassie-stained gel is shown to the right. Molecular weight (MW) markers are indicated. Scale bars, 10 µm (whole cells) and 1 µm (insets). Whole cell images shown are maximum intensity projections of z-stacks containing 64 planes, and inset images shown are projections from 2 to 4 planes.

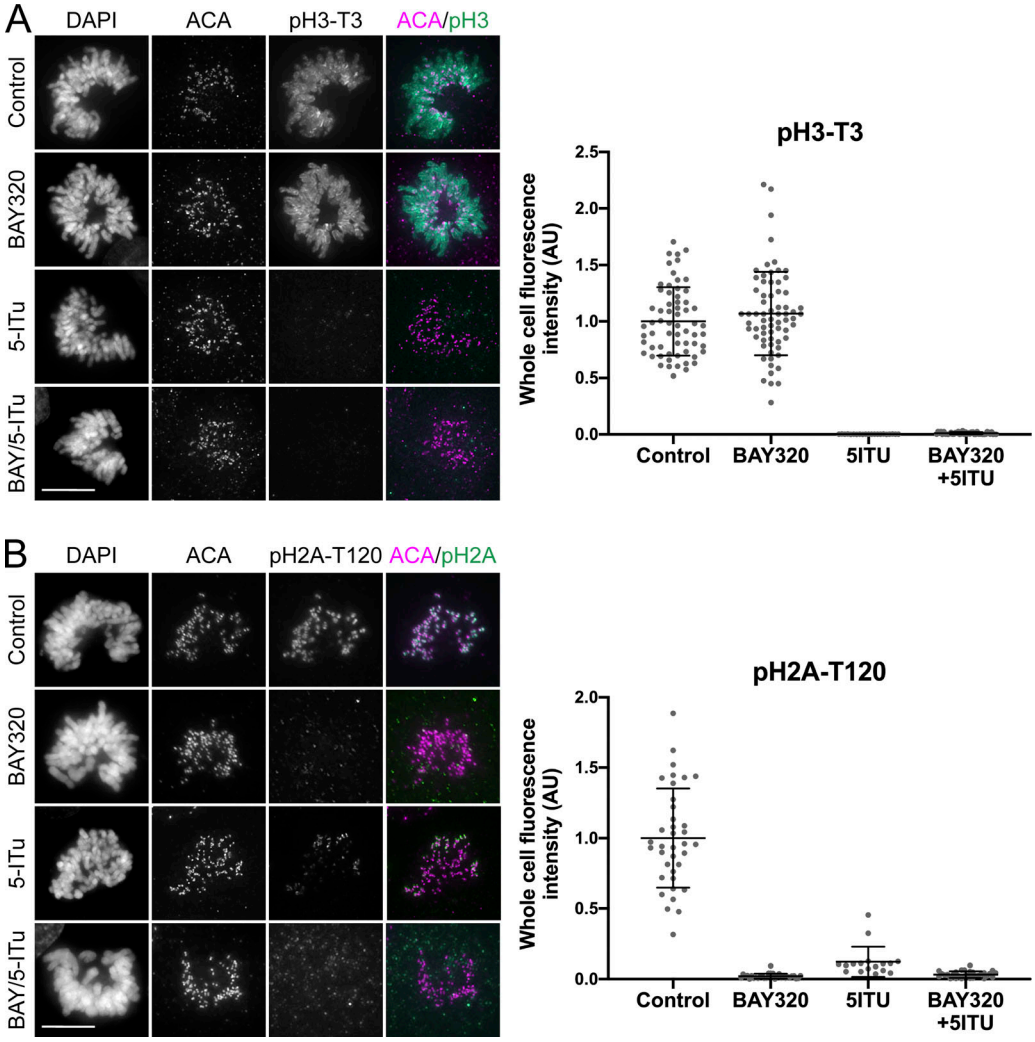

Figure S4. **Specificity of Bub1 and Haspin kinase inhibitors. (A)** Immunofluorescence images of control HeLa cells and cells treated with 10 µM BAY320, 10 µM 5-ITu, or both kinase inhibitors for 30 min and then immunostained for pH3-T3. Quantification of whole cell fluorescence intensity for each condition is shown to the right. Fluorescence intensities for test conditions were normalized to those calculated from control cells. For all conditions, at least 16 cells from three independent experiments were measured. Error bars indicate SD. **(B)** Immunofluorescence images of control HeLa cells and cells treated with 10 µM BAY320, 10 µM 5-ITu, or both kinase inhibitors for 30 min and then immunostained for pH2A-T120. Quantification of whole cell fluorescence intensity for each condition is shown to the right. Fluorescence intensities for test conditions were normalized to those calculated from control cells. For all conditions, at least 14 cells from three independent experiments were measured. Error bars indicate SD. Significance values were calculated using a one-way ordinary ANOVA test. Shown are significance values between each experiment and control cells. Scale bars, 10 µm. AU, arbitrary units.

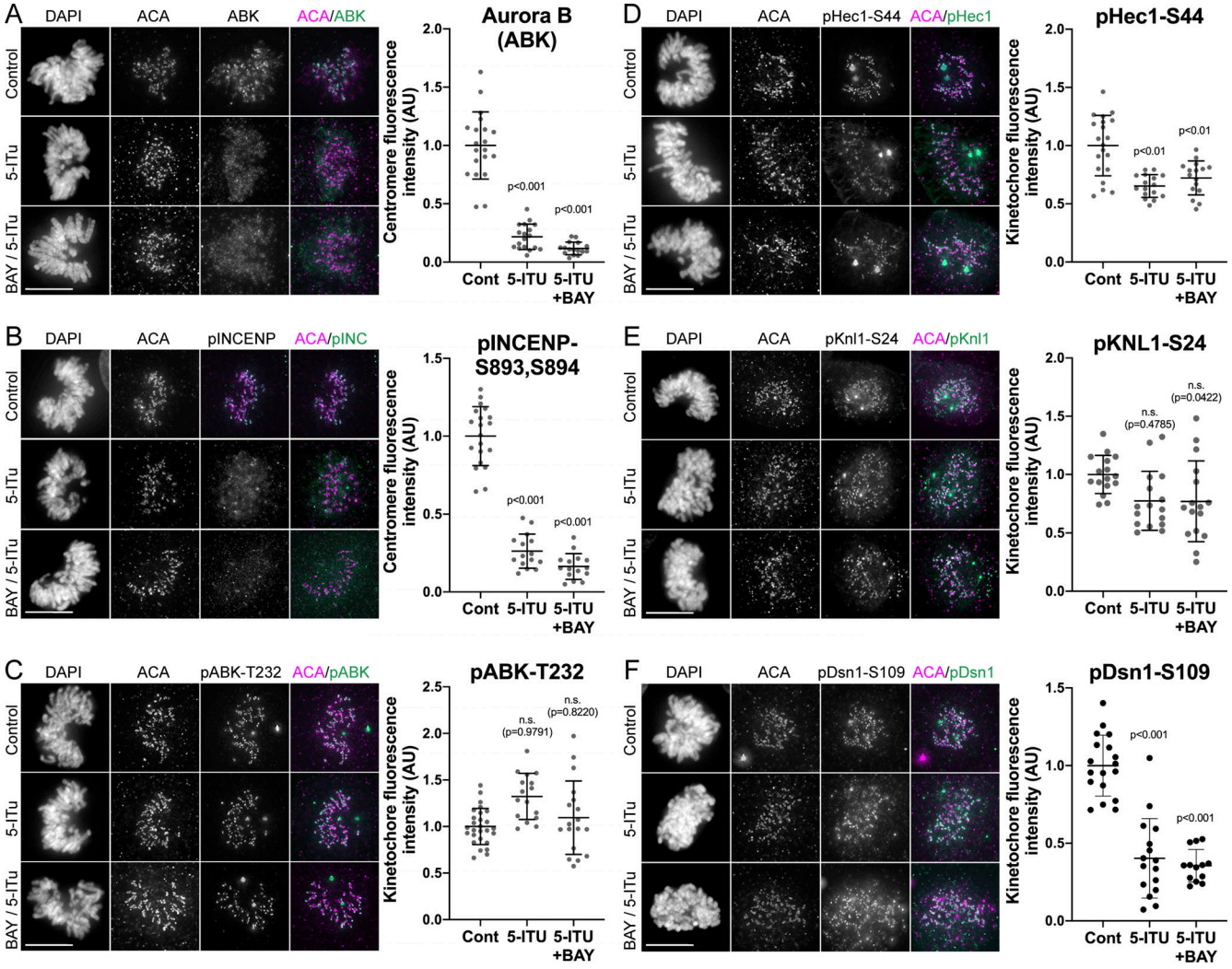

Figure S5. **5-ITu treatment prevents accumulation and activity of Aurora B at centromeres, but not kinetochores. (A–F)** Immunofluorescence images of control HeLa cells or HeLa cells treated with either 10 µM 5-ITu or 10 µM 5-ITu plus 10 µM BAY320 for 30 min. Cells were fixed and stained with the indicated antibodies. To the right of each immunofluorescence panel is the quantification of fluorescence intensities. Fluorescence intensities for test conditions were normalized to those calculated from control cells. *n* values for each experiment follow. ABK: Control (*n* = 153 centromeres; 15 cells; four experiments); 5-ITu (*n* = 161 centromeres; 14 cells; three experiments); 5-ITu + BAY320 (*n* = 115 centromeres; 11 cells; three experiments). pINCENP: Control (*n* = 349 centromeres; 15 cells; three experiments); 5-ITu (*n* = 210 centromeres; 10 cells; three experiments); 5-ITu + BAY320 (*n* = 195 centromeres; 10 cells; three experiments). pABK-T232: Control (*n* = 621 kinetochores; 42 cells; four experiments); 5-ITu (*n* = 359 kinetochores; 38 cells; four experiments); 5-ITu + BAY320 (*n* = 279 kinetochores; 40 cells; four experiments). pHec1-S44: Control (*n* = 384 kinetochores; 16 cells; three experiments); 5-ITu (*n* = 374 kinetochores; 16 cells; three experiments); 5-ITu + BAY320 (*n* = 336 kinetochores; 16 cells; three experiments). pKnl1-S24: Control (*n* = 363 kinetochores; 16 cells; three experiments); 5-ITu (*n* = 337 kinetochores; 16 cells; three experiments); 5-ITu + BAY320 (*n* = 309 kinetochores; 18 cells; three experiments). pDsn1-S109: Control (*n* = 400 kinetochores; 18 cells; three experiments); 5-ITu (*n* = 295 kinetochores; 16 cells; three experiments); 5-ITu + BAY320 (*n* = 315 kinetochores; 16 cells; three experiments). Error bars represent SD. Significance values were calculated using a one-way ordinary ANOVA test. Shown are significance values between experiments for each test condition compared with control cells. Scale bars, 10 µm. AU, arbitrary units.